NASA-CR-194861

Final Report on NASA Contract NAGW-2130

A. Title: An Analysis of Solar Mesospheric Temperatures for the Upper Stratosphere and Mesosphere

B. Principal Investigator: Dr. R. Todd Clancy
Co-Investigator: Dr. David W. Rusch
both at Laboratory for Atmospheric and Space Physics
University of Colorado
Boulder, CO 80309

C. Abstract of Research Objectives:

We proposed to analyze Solar Mesosphere Explorer (SME) limb profiles of Rayleigh scattered solar flux at wavelengths of 304, 313, and 443 nm to retrieve atmospheric temperature profiles over the 40-65 km altitude region. These temperatures can be combined with the previous analysis of SME 296 nm limb radiances (Clancy and Rusch, 1989) to construct a monthly average climatology of atmospheric temperatures over the 40-90 km, upper stratosphere-mesosphere region, with ~4 km vertical resolution. We proposed to investigate the detailed nature of the global temperature structure of this poorly measured region, based on these 1982-1986 SME temperatures. The average vertical structure of temperatures between the stratopause and mesopause has never been determined globally with vertical resolution sufficient to retrieve even scale-height structures. Hence, the SME temperatures provided a unique opportunity to study the detailed thermal structure of the mesosphere, in advance of Upper Atmosphere Research Satellite (UARS) measurements and the Thermosphere Ionosphere Mesosphere Energy and Dynamics (TIMED) mission.

D. Summary of Results:

The SME temperature analysis was completed in early 1993, and we have completed a manuscript describing these temperatures, submitted to the Journal of Geophysical Research in October of 1993. A preprint of this manuscript is attached to this report. The key thrusts of this publication are a comparison of the SME upper stratosphere-mesosphere temperature climatology to the standard CIRA 86 temperature climatology (Fleming et al., 1990) of the same region, and the identification of a distinct, middle mesosphere (75-80 km) temperature minimum which appears at winter midlatitudes and at equinoctal low latitudes. This feature is suggested in the CIRA 86 climatology, which does not possess sufficient vertical resolution to indicate the true vertical extent and location of the temperature minimum. We also compare the SME climatology to various ground-based lidar measurements of mesospheric temperatures, which have observed and interpreted this midlatitude temperature feature at 40-44°N (e.g., Hauchecorne et al., 1987) as a mesosphere temperature inversion. We find a closer association of the winter midlatitude and equatorial temperature minima with the stratopause-mesopause semiannual oscillation (SAO). The enhanced vertical structure of SME mesospheric temperature profiles appears to lead to seasonally and latitudinally dependent biases between the CIRA 86 and SME mesospheric temperatures, which are 5-10 K in the lower mesosphere and 10-25 K in the upper mesosphere. Part of this difference may also represent temporal variability in the 2-4 year average thermal structure of the mesosphere, since the CIRA 86 climatology is based on 1973-1978 measurements and the SME climatology is based on 1982-1986 measurements.

E. Conference Presentation:

Global Middle Atmospheric (20-100 km) Temperatures Derived from Satellite Ultraviolet, Visible, and Near-Infrared Limb Profiles of Rayleigh Scattering, R.T. Clancy and D.W. Rusch, 5th Topical Meeting, Optical Remote Sensing of the Atmospheres, Nov. 18-21, Williamsburg, VA., 1991.

F. Journal Publications:

Solar Mesosphere Explorer Temperature Climatology of the Mesosphere as Compared to the CIRA Model, .T. Clancy and D.W. Rusch, Adv. Space Res., 10, 12,187-12,206, 1990.

Temperature Minima in the Average Thermal Structure of the Middle Mesosphere (70-80km) from Analysis of 40-93 km SME Global Temperature Profiles, R.T. Clancy, D.W. Rusch, and M. T. Callan, J. Geophys. Res., submitted, 1993.

Temperature Minima in the Average Thermal Structure of the Middle Mesosphere (70-80 km) from Analysis of 40-92 km SME Global Temperature Profiles

by

R. Todd Clancy, David W. Rusch, and Michael T. Callan

Laboratory for Atmospheric and Space Physics

University of Colorado

Boulder, CO 80309

Submitted to JGR Atmospheres
December, 1993

Abstract

Global temperatures have been derived for the upper stratosphere and mesosphere from analysis of Solar Mesosphere Explorer (SME) limb radiance profiles. The analysis of additional SME wavelength radiances at 304, 313, and 442 nm provides for extension of the original SME 60-90 km temperature climatology (Clancy and Rusch, 1989a) to a much expanded altitude coverage of 40-92 km. The SME temperatures represent fixed local time observations at 2-3 pm, with partial zonal coverage of 3-5 longitudes per day over the 1982-1986 period. These new SME temperatures are compared to the CIRA 86 climatology as well as individual lidar and rocket observations. Significant areas of disagreement between the SME and CIRA 86 mesospheric temperatures are 10 K warmer SME temperatures in the 55-65 km altitude region and 10-20 K warmer SME temperatures at altitudes above 80 km. Although much of this disagreement probably stems from the poor vertical resolution of the CIRA 86 model and the limited local time and longitudinal coverage of the SME temperatures, some portion of the differences may reflect 5-10 year temporal variations in mesospheric temperatures. The SME temperatures also exhibit enhanced amplitudes for the semiannual oscillation (SAO) of upper mesospheric temperatures at low latitudes, which are not evident in the CIRA 86 climatology. The so-called mesospheric "temperature inversions" at wintertime midlatitudes, which have been observed by ground-based lidar (Hauchecorne et al., 1987) and rocket *in situ* measurements (Schmidlin, 1976), are shown to be a climatological aspect of the mesosphere, based on the SME observations. The winter midlatitude "temperature inversion" is evident in both winter hemispheres and appears more distinctly as a low altitude (75 km) temperature minimum at southern midlatitudes . Furthermore, the SME temperatures indicate the related presence of low latitude temperature minima at 80 km altitude during the equinoxes. Both the low latitude semiannual minima and the midlatitude annual minima in middle mesospheric temperatures appear to result from the strong SAO in mesospheric temperatures.

Introduction

Global observations of the upper stratospheric and mesospheric temperatures recently have been obtained from several Upper Atmospheric Research Satellite (UARS) experiments and are planned with the upcoming Thermospheric Ionospheric Mesospheric Energetics and Dynamics (TIMED) mission. As both a reference and a baseline for long-term and interannual variations in the thermal structure of the upper middle atmosphere, we present a composite global climatology of Solar Mesosphere Explorer (SME) atmospheric temperatures in the 40-92 km altitude region. The SME temperatures are derived from Rayleigh limb scattering profiles as observed between 1982 and 1986. This new SME climatology extends the altitude range of the previously published SME upper mesospheric temperatures (Clancy and Rusch, 1989a) through the entire mesosphere and upper stratosphere, based on analysis of longer wavelength ultraviolet (304, 313 nm) and visible (442 nm) limb scattering observations from SME. Global definitions of mesospheric temperatures prior to the SME observations have been based on the accumulated statistics of rocket measurements obtained over an extended period of time (CIRA 1972) or global nadir soundings within the 15 micron CO_2 band (the basis for the Middle Atmospheric Program, or MAP, climatology, Barnett and Corney, 1985). The CIRA 1972 climatology suffered from the restricted global coverage and quantity of the rocket observations. The MAP climatology is affected by the limited vertical resolution (12-20 km) of nadir infrared sounding. The new CIRA 1986 climatology (Fleming et al., 1990) incorporates the MAP model up to an altitude of 80 km, and the MSIS 83 thermospheric model for altitudes between 86 and 120 km (Hedin, 1983). We employ this model as a standard of comparison for the SME temperatures over the 40-92 km altitude range.

The SME temperatures exhibit the advantages of full seasonal, 40°S-40°N latitudinal coverage (and up to 75°S-75°N for a reduced range of seasons) over an extended period of time (4-5

years), and relatively high vertical resolution (4 km) from a fixed local time (2-3 pm) of observation. The enhanced altitude range of the new SME temperatures provides unique seasonal coverage of the stratopause and mesopause regions with sub-scale height vertical resolution. We indicate aspects of these SME temperatures which suggest that distinct temperature minima in the average mesosphere profile descend to altitudes below 85 km for certain seasons and latitudes. These minima include the temperature inversion feature identified at 40-45°N during winter (Schmidlin et al., 1976; Hauchecorne et al., 1987; Meriwether et al., 1993), as well as its related behavior at winter southern midlatitudes (Clancy and Rusch, 1989a), and semiannually varying features at equatorial latitudes. Where comparisons are possible, we indicate agreements and disagreements between the SME temperature climatology and the CIRA 86 climatology, monthly averaged rocket measurements over a limited number of sites, and lidar sites. Of particular interest are the latitudes and seasons during which these middle mesospheric temperature minima appear.

SME Observations

The SME limb profiles of Rayleigh scattered solar flux at ultraviolet and visible wavelengths have been described by Rusch et al. (1984) and Mount et al. (1984), respectively. The inversions of these limb profiles to volume scattering for studies of atmospheric temperatures and aerosol scattering are described in detail in Clancy and Rusch (1989a) and Clancy (1985). The essential aspects of the SME limb scattering profiles are provided in figure 1, which presents SME limb profiles at wavelengths of 296, 304, 313, and 442 nm. The exponentially increasing portions of the limb radiance profiles correspond to Rayleigh scattering from the exponentially increasing density of the molecular atmosphere coupled with the limb geometry of the observations. The ultraviolet limb profiles exhibit radiance maxima at altitudes of 40-60 km due to wavelength-dependent ozone absorption in the Hartley band (Rusch et al., 1984). The 442 nm limb profile reaches a maximum below 30 km as the slant path molecular and aerosol scattering extinction

opacities approach unity (Clancy, 1986). Both the visible and ultraviolet limb radiances are inverted to yield volume radiance profiles, based on the known limb geometry, the instrumental field-of-view, and a least-squares matrix inversion algorithm (see Clancy and Rusch, 1989a). For the altitude portions of these profiles over which the limb extinction (ozone absorption or molecular scattering) opacity is less than a few percent it is possible to derive atmospheric temperatures with the assumption of hydrostatic equilibrium, the ideal gas law, and the absence of aerosol scattering. During the solstice seasons, the SME temperatures are restricted to <55° latitudes by the absence of sunlight over winter high latitudes, and by the presence of polar mesospheric clouds (e.g., Thomas , 1984) over summer high latitudes.

The contribution of aerosol scattering in the lower stratosphere during the SME period of observations is dominated by the El Chichon eruption (e.g., Thomas et al., 1983). As shown in Clancy (1986), the SME 442 nm limb measurements demonstrate the penetration of significant El Chichon aerosol scattering to altitudes as high as 40 km approximately 6 months after the eruption. This in fact determines the lower limit for the derivation of SME temperatures presented in the current work. The upper altitude limit for the SME temperature analysis is determined by the signal-to-noise ratios of the SME limb radiance profiles, which also constrain the temporal resolution of the derived temperatures. The SME limb radiances are summed into monthly averages in order to achieve sufficiently high signal-to-noise ratios (>100) over the entire altitude range of analysis. Although daily temperature profiles have been calculated over reduced altitude ranges, the limited longitudinal coverage of the SME observations is better suited to derivation of monthly average temperatures. Upper altitude limits for the 296, 304, 313, and 442 nm radiance derivations of temperature are 93, 86, 86, and 54 km respectively. The lower altitude limits for the 296, 304, and 313 nm radiance determinations of temperature are 66, 58, and 54 km respectively, as set by a maximum ozone extinction opacity of .02 in the limb viewing geometry.

The 1982-1986 period of SME limb observations encompasses daily limb measurements at 296 and 442 nm for 3-5 widely separated longitudes. Figure 2a presents the SME longitudinal

coverage between 1982 and 1986 at these wavelengths. The 304 and 313 nm limb observations were obtained from 1983-1986, and are limited to longitudes in the western hemisphere (figure 2b). Although the monthly averaged aspect of the SME temperatures dampens much of the zonal variability introduced by the incomplete zonal coverage of SME, there remain potential sampling biases which we consider in the temperature comparisons presented below. Measurement uncertainties in the SME temperatures are detailed in Clancy and Rusch (1989a). They are dominated by reduced signal-to-noise ratios at altitudes above 80 km altitude, which lead to ± 10K errors (1σ) for monthly average temperatures at 90 km altitude. At altitudes below 80 km the primary error sources are profile inversion errors (± 2K), altitude uncertainties (± 2K), and the effects of ozone absorption at the lowermost altitudes of inversion. This last term led to underestimations of ~5 K in the SME 296 nm temperatures presented in Clancy and Rusch (1989a) for altitudes near 60 km. In this current analysis, we further restrict the lower altitude range of temperature retrieval for each wavelength channel to remove the effects of ozone absorption on the temperature derivations (as indicated above).

SME-CIRA 86 Comparisons

We employ the CIRA 86 climatological model of middle atmospheric temperatures as the basis of comparison for our presentation of the SME temperatures. The CIRA 86 monthly average temperature profiles in the 20-80 km altitude range are a synthesis of nadir IR (CO_2) sounding observations obtained by the Nimbus 7 Selective Chopper Radiometer (SCR, Ellis et al., 1973) experiment in 1973-1974 and the Nimbus 6 Pressure Modulated Radiometer (PMR, Curtis et al., 1974) experiment in 1975-1978. Both sets of observations obtained global (80°S-80°N, full zonal) measurements over these time periods. The SCR data are used to define the CIRA 86 climatology below 40-50 km , the PMR data define the CIRA 86 climatology between 50 and 80 km altitude. At altitudes above 86 km, the CIRA 86 climatology is derived from the thermospheric empirical model MSIS 83, which includes a variety of spacecraft observations of the

thermosphere versus solar activity. However, the MSIS model over the 86-100 km region is primarily an extrapolation from the 120 km altitude level (Hedin, 1983). The SCR and PMR temperature retrievals provide vertical resolutions which vary from 12 km in the lower stratosphere to 20 km in the upper mesosphere (Barnett and Corney, 1985). The CIRA 86 climatology has become a fairly standard representation of the background middle atmosphere for both data analysis of observations lacking contemporaneous temperature measurements and for modelling of photochemistry (e.g., Clancy et al., 1993), particularly for the mesosphere where the long-term National Meteorological Center (NMC) temperatures are not available. Hence, we stress the distinctions between the SME and CIRA 86 mesospheric temperatures as an indication of the existing uncertainties in the background temperature field of the mesosphere. As the following SME-CIRA comparisons indicate, there exist large differences (5-20 K) in the inferred background temperatures of the mesosphere which exhibit distinctive temporal, vertical, and latitudinal structures. The key issues regarding the SME-CIRA temperature comparisons are the limited vertical resolution of the CIRA mesospheric temperatures, the restricted longitudinal and local time coverage of the SME mesospheric temperatures, and potential temporal (timescale>4-5 years) changes in the temperature field of the mesosphere.

In figures 3-7 we present profiles of the composite SME temperatures (dashed lines) and CIRA 86 (solid lines) temperatures for latitudes of 40°N, 15°N, 0°, 15°S, and 40°S for the months of January, April, July, and October. The SME temperatures indicate both the individual wavelength measurements (as various symbols) and the interpolated composite SME temperature profile formed over the full 40-92 km altitude range of the SME temperature measurements. The SME composite profiles of temperature are computed as a least-squares, sliding cubic spline fit through the individual wavelength measurements. The variations in SME temperatures present among multiple wavelength measurements of temperature at a given altitude are partly due to the 2-5 K uncertainties in the SME temperature retrieval at altitudes below 86 km. It is also possible that the different longitudinal coverages represented among the different wavelength channels (see figure 2) lead to biases in the monthly average temperatures, even for the 3-4 year averages

represented by these SME temperatures. The SME 304 and 442 nm temperature measurements at 55 km altitude, in particular, display a consistent offset with respect to one another of ~5 K. This bias is probably due to the fact that the 55 km altitude corresponds to the lower and upper boundaries of temperature retrieval for the 304 and 442 nm channels, respectively.

The differences between the SME and CIRA 86 mesospheric temperatures can be roughly characterized by three cases. The first case regards the strong semiannual oscillation (SAO) of equatorial mesopause temperatures which is evident in both the SME and CIRA 86 temperatures (figures 4-6). The SME definition of the SAO in the mesosphere, based on the earlier analysis of 296 nm limb radiances (Clancy and Rusch, 1989a), exhibits an increasing amplitude for the mesosphere SAO up to 90 km altitude at equatorial latitudes (Garcia and Clancy, 1991). The CIRA 86 climatology includes very little mesosphere SAO amplitude above 85 km altitude where the MSIS 83 model is applied, but significant amplitudes below 85 km where the MAP IR-based model is employed. Furthermore, the mesosphere SAO vertical wavelength (~20 km) is not well sampled by the 20 km vertical resolution of the MAP temperatures in this region. The comparisons between the equatorial SME and CIRA 86 temperatures of figures 4-6 suggest that the limited vertical resolution of the CIRA 86 measurements at altitudes above 60 km do not adequately resolve the strong SAO variations and may lead to complex biases in the vertical temperature profiles for this region. Alternatively, the constant local time (2 pm) of the SME climatology may lead to biases from strong tidal variations in temperatures near the equator. Based on current tidal models, the phases of the diurnal tides are not predicted to vary seasonally and the amplitude of the diurnal tide is predicted to decrease to near zero at 15° north and south of the equator (Forbes and Gillette, 1982), suggesting that tidal variations in mesospheric temperatures are not the primary cause of the large SAO signature in the 15°S-15°N SME temperature climatology above 80 km altitude. However, few observations are available to support the tidal models in such detail, and tides undoubtably influence comparisons between the SME and CIRA 86 climatologies. In any case, the CIRA 86 and SME climatologies exhibit disagreements as large as 20 K near the equatorial mesopause around the equinoxes (e.g., figures 5b and 5d). The meso-

spheric SAO signature in the SME temperatures effectively leads to a deep temperature minimum, near the equinoxes, at an altitude of ~80 km. The CIRA 86 climatology present weaker temperature inflections near 70 km for the same seasons.

Similarly, the SME mesospheric temperatures present a striking wintertime minimum near 75 km at midlatitudes (figures 3c and 7a), which is far less distinct, although suggested, in the CIRA 86 temperatures. This feature was originally described as a wintertime temperature inversion of variable intensity within the mesosphere, based upon rocket observations (Schmidlin, 1976) and groundbased lidar observations over Haute Province (Hauchecorne et al., 1987). It has also been observed by ground based lidar over Wright Patterson AFB in Ohio (Meriwether et al., 1993), as well as in the earlier SME temperature analysis (Clancy and Rusch, 1989a). The SME climatology indicates that this feature exists in the southern as well as northern midlatitude winter, that it characterizes the monthly average temperature profile, and that it appears more distinctly as a mesospheric temperature minimum in the southern hemisphere (c.f. figures 3c and 7a). In fact, this feature appears related to the equatorial temperature minimum in its behavior, within both the CIRA 86 and SME climatologies. However, the midlatitude temperature minima exhibit more annual character, and descend to a lower altitude (~75 km), as we describe in more detail below. The differences between the SME and CIRA 86 characterizations of these midlatitude minima are also quite similar to those exhibited for the SAO temperature minima near 80 km (figures 4-6 b and d).

The third area of disagreement between the SME and CIRA 86 climatologies regards the generally warmer lower mesosphere indicated by the SME versus the CIRA temperatures. SME temperatures are typically 10K warmer than CIRA 86 temperatures over the 55-65 km altitude region, as can be seen from figures 4-8. This distinction was not apparent in the earlier SME temperature analysis (Clancy and Rusch, 1989a), which did not provide temperature retrieval below 58.5 km. Furthermore, the 58.5-62 km SME temperatures from the 296 nm limb radiances were biased low by incomplete correction for ozone absorption. The 304 and 313 nm temperature derivations for the lower mesosphere are not sensitive to ozone absorption due to the much re-

duced ozone absorption cross sections at these wavelengths. Consequently, the new composite SME temperature profiles presented here provide the first reliable comparison of CIRA and SME temperatures in the lower mesosphere. The distinctions between lower mesospheric temperatures from the SME and CIRA 86 climatologies may partly arise from the differences at higher altitudes, where the vertical location of the middle mesosphere temperature minimum is offset between the two climatologies. Comparisons with rocket and lidar measurements of temperatures are provided below to assess the relative accuracies of the SME and CIRA 86 climatologies in this region. Far fewer comparisons are available at altitudes above 80 km.

A portion of the disagreement between these SME and CIRA 86 temperatures must be due to vertical resolution effects in the CIRA temperatures between the cold mesopause and the warm stratopause. This effect becomes even more important if the identification of a distinct, seasonally and latitudinally dependent temperature minimum in the middle mesosphere is proved correct. The vertical resolution of the CIRA measurements is not sufficient to resolve the stratopause without prior constraints on the stratopause altitude and shape, and CIRA 86 is very model dependent in the mesopause region. On the other hand, the incomplete zonal coverage of the SME measurements may contribute to differences in the lower mesospheric temperatures and the stratopause altitude. SME temperatures also do not extend above 92 km altitude and were obtained for a fixed local time, such that complex double mesopause structures at higher altitudes (e.g., She et al., 1993; Bills and Gardner, 1993) and the effects of tides cannot be separately identified. Furthermore, the different time periods of the observations reflected in the SME and CIRA 86 temperatures may lead to real differences, given that temperature trends of >5K over 3-5 year periods are observed for the upper stratosphere (Clancy and Rusch, 1989b) and the mesosphere (Clancy and Rusch, 1989a; Chanin et al., 1987). In the following sections, we present comparisons of the SME temperatures to local rocket and lidar profiles of 40-90 km temperatures, followed by a comparison of the middle mesosphere temperature minima regions from the SME and CIRA 86 temperature data sets.

SME-Rocket Comparisons

A fairly large set of datasonde temperature measurements were obtained during 1982, which are appropriate for comparison to SME lower mesospheric temperatures at 4 separate locations. These sites (Pt. Mugu, CA; Wallops Island, VA; Ascension Island; and Barking Sands, HI) range from 10°S to 37°N in latitude and include measurements for the months of January and March of 1982. The averaged datasonde temperatures for each location, which incorporate 8-29 separate flights per monthly average, are presented in figures 8 a-f as asterisk symbols with error bars. The average local times of the rocket observations are 2-7 pm, as indicated on each figure. The error bars presented for each rocketsonde profile present $\pm$ 1σ in the observed distributions of temperatures at each site. SME and CIRA 86 temperature profiles are included for comparison as dashed and solid lines, respectively. In general, the datasonde temperatures in the 55-65 km altitude range are warmer by ~10K than the CIRA 86 temperatures, and in much better agreement with the SME temperatures in this same region.

Specifically, the average difference in the rocket versus SME temperatures is less than 5K between altitudes of 48 and 72 km. The average of the six rocket temperatures is 13K warmer than CIRA 86 at 60 km. There have been recent indications of bias errors in datasonde temperatures above 60 km altitude. Based on comparisons between falling sphere and datasonde temperature measurements, Schmidlin et al. (1991) suggest that datasonde temperature measurements at ~65 km may be biased high by ~5 K, with significantly increasing biases above this altitude. At and below 60 km altitude, the falling sphere and datasonde temperatures exhibited agreement to better than 3 K. Hence, the agreement between SME and the datasonde profiles and their disagreement with CIRA 86 near 60 km is not significantly impacted by the reported errors in datasonde mesospheric temperature measurements.

At altitudes above 70 km, comparisons of the datasonde temperatures with the CIRA 86 and SME temperatures are subject to potentially large bias errors in the datasonde measurements. Nevertheless, it is of interest to note that the March datasonde profiles at the low latitude stations

suggest the presence of local temperature minima near 80 km altitude. Specifically, low-altitude temperature minima present in the March 10°S and 20°N SME profiles of figures 8b and 8c are suggested in the accompanying Ascension Island and Barking Sands profiles. Furthermore, the January Pt. Mugu profile of figure 8d suggests a temperature minimum near 75 km which compares reasonably well with the 74 km temperature minimum presented in the comparison SME temperature profile.

SME-Lidar Comparisons

In figures 9 a-f, we present comparisons of the 45°N latitude SME temperature climatology (dashed lines) to the Haute-Provence, France (44°N, 6°E) lidar temperature observations, for every other month. In each case, we include the French monthly averaged profiles for the 1981-1984 period (dotted lines, from Chanin et al., 1985) and for the 1981-1987 period (solid lines, from Chanin et al., 1990). For several months, notably July and November, there exist significant differences between these two period averages. The lidar temperatures are nighttime measurements, and incorporate roughly 30-50 observations per monthly average for the 1981-1987 averages, and roughly half that for the 1981-1984 averages. The upper altitude limit of these French lidar measurements is 80 km, where the predicted (e.g., Forbes and Gillette, 1982) solar tidal variations at 80 km, 40° latitude are ~5 K in amplitude. Hence, the 2 pm SME observations and the nighttime lidar observations could represent atmospheric temperatures that are intrinsically distinct by 2-5 K at altitudes between 70 and 80 km due to diurnal temperature variations. Such differences are within the uncertainties of our comparisons, given the different longitudes sampled by the SME and lidar comparisons (e.g., see Clancy and Rusch, 1989a). However, the effects of solar tidal variations in mesospheric temperatures become a more significant issue at higher altitudes and equatorial latitudes, as we discuss below.

The lidar (1981-1984)-SME comparisons of figure 9 indicate agreement of better than 5 K except for January , May at 60 km and March at 45 km, where 5-10 K disagreements are found.

The 1981-1987 lidar temperatures are 4-7 K colder than the SME temperatures at 55-65 km altitude for the yearly average. The lidar temperatures are typically 6-7 K warmer than the CIRA 86 temperatures at 55-65 km over the 1981-1984 period, and 3-4 K warmer for the full 1981-1987 period, indicating cooling in this region between 1981 and 1987. Agreement above and below the 55-65 km region is typically within 3 K among the lidar, SME, and CIRA 86 temperatures.

More recent lidar observations by Bills and Gardner (1993) allow a comparison with SME temperatures above 80 km, at 40°N latitude (Urbana, Illinois- 88°W). In figures 10 a and b, we present the seasonal (January-June) variation of atmospheric temperatures at 85 and 90 km, respectively, for the SME (crosses), Urbana lidar (solid line), and CIRA 86 (asterisks) data sets (see also figures 7a and 7b). As with the French lidar observations, the Urbana data are nighttime measurements. The SME and Urbana lidar temperatures exhibit very similar seasonal trends in 85-90 km atmospheric temperatures over the January-June period, whereas the CIRA 86 climatology presents considerably smaller seasonal variation, particularly at 90 km altitude. The CIRA 86 temperatures agree better in an absolute sense with the Urbana lidar measurements at 85 km, but exhibit a 5-15 K cooler temperatures at 90 km. The SME temperatures are 10 K warmer than the Urbana temperatures at 85 and 90 km, for the entire January-June period.

The relatively constant 10 K difference between the SME and Urbana lidar temperatures at 85-90 km may be partly explained by solar tidal variations as well as the distinct longitudinal and temporal coverages and measurement uncertainties for the two data sets. The Forbes and Gillette (1982) tidal model predicts diurnal and semidiurnal amplitudes of 4-6 K at 87 km, 40° latitude, with a constant phase (versus season), except for the semidiurnal tide during winter solstice. Atmospheric temperatures at 85-90 km for the local time of the SME measurements would be ~5-10 K warmer than for the nighttime period corresponding to the lidar observations, based on the Forbes and Gillette model. Gille et al. (1991) derived tidal temperature variations at 44°N with the Haute Provence lidar up to 80 km altitude, which exhibit distinctions from the Forbes and Gillette model, but still suggest that the local time of the SME measurements would lead to ~5 K warmer temperatures near 80 km than would be observed at nighttime. The CIRA 86 model

incorporates a diurnal average calculation from the MSIS 83 model, which characterizes CIRA temperatures above 80 km. The Urbana temperatures also indicate a relatively low altitude (86 km) for the mesopause in June, which is in agreement with the SME temperature profile for June, 40°N.

Our final lidar comparison is with the high latitude (69°N) Andenes, Norway site for which Lubken and von Zahn (1991) have combined both lidar and *in situ* measurements to obtain monthly mean temperature profiles for nine months of the year. Comparisons with SME temperature profiles can be obtained only for the months of October and March at 70°N, and August at 65°N due to the presence of noctilucent clouds around summer solstice and polar nighttime conditions around the winter solstice. We present comparisons between the Norway (heavy dash-dotted lines), the CIRA 86 (solid lines), and the SME temperature profiles (symbols and dashed lines) for these three cases in figures 11 a-c. Qualifications regarding the different local times among these data sets apply as described above, although tidal variations are presumed to be smaller at this higher latitude.

Middle Mesosphere Temperature Minima

In order to investigate potential processes that may be responsible for the middle mesosphere temperature minima, we plot the annual variations in the SME (heavy lines) and CIRA 86 (light lines) temperatures at 75 (solid) and 85 (dashed) km altitudes. Figure 12a presents these temperatures for the latitude range 5°S-5°N, and figure 12b presents the latitude range 30°S-40°S. In these plots, the middle mesospheric temperature minima are characterized as periods when the 75 km temperature is colder than the 85 km temperature. In figure 12a (equatorial latitudes), the months of April and October are shown to be periods when temperature minima are observed at altitudes near 80 km. The development of the minima reflects the strong semiannual variations in both the 75 and 85 km temperatures, and the fact that the semiannual variations at these two altitudes are completely out-of-phase. Hence the equatorial middle mesosphere temperature minima

appear to be a consequence of the strong semiannual oscillation within the low-latitude mesosphere [see Garcia and Clancy (1990) for the discussion of the mesosphere SAO; and Clancy and Rusch (1990) for a spectral analysis of the annual and semiannual variations in the 60-90 km SME and CIRA 86 temperatures]. Although the signal-to-noise ratios of daily average temperatures computed from SME limb radiances are poor, we have computed such temperatures (not shown) to determine whether the temperature minima in the middle mesosphere are influenced by extreme temperatures within an anomalous event, such as reported by Meriwether et al. (1993). We find that the annual variations presented in figures 12a and 12b are representative of the daily temperatures, rather than singular conditions such as stratospheric warmings.

One other interesting aspect of the SAO variations in figures 12a and b is the noticeably stronger SAO variation for the second (October) versus the first (April) equinoctial season. This behavior is also reflected in the lower altitude of the middle mesosphere minimum from October versus the April temperature profiles presented in figures 4-6. The seasonal asymmetry of the stratopause SAO has been noted by Delisi and Dunkerton (1988), and is attributed to northern hemisphere planetary wave activity during the winter. However, they derive larger SAO wind amplitudes for the first equinoctial season (April). In fact, the SME temperatures also exhibit a larger SAO temperature amplitude for April at lower altitudes (60-70 km), as indicated in Garcia and Clancy (1990).

Strong diurnal tides, which are predicted at altitudes above 80 km near the equator, must also impact the interpretation of figure 12a to some level, particularly if they prove to vary strongly with season. However, the basic character of the SME temperatures presented for latitudes 5°S-5°N in figure 12a remain essentially the same out to 20°S and N latitudes [e.g., figures 4 and 6, see also Clancy and Rusch (1990)]. In contrast, the diurnal tide is predicted to decrease to zero near 18°NS [e.g., Forbes and Gillette (1982)]. The CIRA 86 temperatures also exhibit semiannual variations for 5°S-5°N, but do not indicate a significant change in the SAO phase between 75 and 85 km altitude, and exhibit very small SAO amplitudes above 80 km altitude. This is partly because the upper mesosphere is sampled with ~20 km vertical resolution by the IR MAP

measurements which form the CIRA climatology below 80 km altitude. Furthermore, the CIRA temperatures are based on a smoothed fit between the MAP temperatures and the MSIS 83 empirical model at altitudes above 80 km. Analysis of equatorial temperatures from 1964-1968 rocketsonde observations (Cole and Kantor, 1975) indicates roughly half the SAO temperature amplitudes determined from SME measurements above 80 km altitude, which is still 2-10 times greater than the SAO in the CIRA 86 model at these altitudes (Garcia and Clancy, 1990).

The midlatitude temperature minima are primarily an annual, wintertime phenomenon, and occur at lower altitudes (~75 km) than the corresponding low latitude minima. Nevertheless, semiannual temperature variations appear to play an important role in the formation of the midlatitude temperature minimum. Near 70 km altitude the amplitude of the annual temperature variation is at a minimum [Clancy and Rusch, 1990], such that the SAO variation dominates the observed temperature variations. This altitude region reflects the transition between the opposite phases of the annual temperature variations within the stratosphere and mesosphere. Both the SME and CIRA 86 temperatures at 75 km (figure 12b) demonstrate the SAO character of midlatitude temperatures in this region. At 85 km altitude both climatologies indicate a strong annual variation in temperatures. The SME temperatures still exhibit significant SAO amplitudes at 85 km, whereas the CIRA 86 temperatures do not. The primary reason that SME temperatures present a midlatitude, wintertime (July in figure 12b) temperature minimum at 75 km while the CIRA 86 temperatures do not, follows from the 15 K average difference between the SME and CIRA 86 temperatures at 85 km. The wintertime temperature minimum in the SME climatology appears to be related to the mesospheric SAO variation, similar to the origin of the equatorial temperature minima. However, at midlatitudes the strong annual variations above 80 km lead to an overall annual, winter character and a lower altitude for the middle mesosphere temperature minimum.

The identification of temperature minima in the climatological structure of the middle mesosphere from the new SME temperatures is made possible by the unique vertical extent and resolution of these measurements. That these temperature minima have not been previously identified

may stem from the incompleteness of previous temperature measurements in this region. Rocket observations are not extensive enough in temporal or global coverage; lidar observations are similarly restricted in coverage and existing systems have only recently provided complete vertical sounding over the key 60-90 km altitude range; and the satellite IR data sets (such as incorporated in CIRA 86) are limited by coarse vertical resolution and an upper altitude limit of ~80 km. Even so, there are indications of such temperature minima structure in the CIRA 86 climatology. Furthermore, the amplitudes of the middle mesosphere temperature minima may vary interannually and over solar-cycle or longer timescales. Mesospheric temperature trends from the earlier 60-90 km SME temperatures between 1982 and 1986 indicated distinct latitudinal and vertical dependences which could alter the intensity of these temperature minima over 5 year timescales (Clancy and Rusch, 1989a). Eleven year trends from the Haute-Provence lidar temperatures also suggest the existence of vertically dependent trends of 1-2 K/yr over 5-10 year timescales (Chanin et al., 1987). Due to the paucity of global measurements in the mesosphere, we cannot be sure of the extent to which differences in temperature characterizations of the mesosphere are due to measurement biases among the techniques or true temporal variability. The mesosphere is predicted to be the most sensitive region to solar cycle as well as long-term variability. Even its annual and semiannual variations are large relative to the stratosphere, and the phase of the annual variation changes by a full 180° between altitudes of 60 and 70 km.

Conclusions

We present an expanded altitude range (40-92 km) for the SME temperature climatology which encompasses the upper stratosphere-mesosphere region (see appendix A). This climatology is compared to the CIRA 86 climatology as well as individual rocket and lidar temperature profiles. Three areas of significant disagreement with the CIRA 86 climatology are a much stronger mesosphere SAO signature in the SME temperatures, particularly above 80 km; 10-20 K warmer temperatures at 80-93 km in the SME versus the CIRA 86 climatology; and 10 K warmer

temperatures at 60 km in the SME versus the CIRA 86 climatology. We argue that many of these differences may result from the poor (20 km) vertical resolution of the IR sounding and MSIS 83 modelling, which form the basis of the CIRA 86 temperatures above 50 km altitude. However, the fixed local time between the SME measurements (2-3 pm) may also lead to significant biases at altitudes above 80 km, particularly at equatorial latitudes. Furthermore, there may exist substantial temporal variations in mesospheric temperatures over 5-10 year timescales which impact the comparison of the CIRA 86 climatology (based on 1973-1978 observations) and the SME climatology (based on 1982-1986 observations).

The SME temperatures indicate the presence of middle mesosphere minima in the average climatological structure of mesospheric temperatures, which form semiannually at 80 km altitude at low latitudes, and form annually at 75 km altitude at midlatitudes. The low latitude minima appear at the equinoxes. The midlatitude features are most marked during the winter, and are equivalent to the wintertime temperature inversions reported by Schmidlin (1976), Hauchecorne et al. (1987), Clancy and Rusch (1989a), and Meriwether et al. (1993). The global SME temperatures suggest that both the equatorial and midlatitude temperature minima are driven by the strong SAO behavior of mesospheric temperatures.

References

Barnett, J. and M. Corney, Middle atmosphere reference model derived from satellite data, in *Handbook for MAP*, Vol. 16, Edited by K. Labitzke, J. J. Barnett, and B. Edwards, pp. 47-137, University of Illinois, Urbana, 1985.

Bills, R. E. and C. S. Gardner, Lidar observations of the mesopause region temperature structure at Urbana, J. Geophys. Res., 98, 1011-1021, 1993.

Chanin, M. L., A. Hauchecorne, and N. Smires, Contribution to the new reference atmosphere from ground-based lidar, in *Handbook for MAP*, Vol. 16, Edited by K. Labitzke, J. J. Barnett, and B. Edwards, pp. 47-137, University of Illinois, Urbana, 1985.

Chanin, M. L., N. Smires, and A. Hauchecorne, Long-term variation of the middle atmosphere at mid-latitude: Dynamical and radiative causes, J. Geophys. Res., 92, 10933-10941, 1987.

Chanin, M. L., A. Hauchecorne, and N. Smires, Contribution to the new reference atmosphere from ground-based lidar, Adv. Space Res., 10, 211-216, 1990.

Clancy, R. T., El Chichon and "mystery cloud" aerosols between 30 and 55 km: Global observations from the SME visible spectrometer, Geophys. Res. Lett., 13, 937-940, 1986.

Clancy, R. T., and D. W. Rusch, Climatology and trends of mesospheric (58-90 km) temperatures based upon 1982-1986 SME limb scattering profiles, J. Geophys. Res., 94, 3377-3393, 1989a.

Clancy, R. T. and D. W. Rusch, The relationship between 1982-1986 trends in upper stratospheric ozone and temperatures, in Ozone in the Atmosphere, R. D. Bojkov and P. Fabian, eds., A. Deepak, Hampton, VA, 822 p., 1989b.

Clancy, R. T., and D. W. Rusch, Solar Mesosphere Explorer temperature climatology of the mesosphere as compared to the CIRA model, Adv. Space Res., 10, 187-206, 1990.

Clancy, R. T., B. J. Sandor, D. W. Rusch, and D. O. Muhleman, Microwave observations and modelling of O_3, H_2O, and HO_2 in the mesosphere, accepted for publication in J. Geophys. Res., 1993.

Cole, A.E. and A.J. Kantor, Tropical atmospheres, 0 to 90 km, Project 8624, AFCRL-TR-75-0527, Aeronomy Laboratory, Air Force Cambridge Research Laboratories, Hanscom, 1975.

Curtis, P. D., J. T. Houghton, G. D. Peskett, and C. D. Rodgers, The pressure modulator radiometer for Nimbus F, Proc. Roy. Soc. London, A337, 135-150, 1974.

Delisi, D.P. and T.J. Dunkerton,m Seasonal variation of the semiannual oscillation, J. Atmos. Sci., 45, 2772-2787, 1988.

Ellis, P. , G. Holah, J. T. Houghton, T. S. Jones, G. Peckham, G. D. Peskett, D. R.en Pick, C. D. Rodgers, K. H. Roscoe, R. Sandwell, S. D. Smith, and E. J. Williamson, The selective chopper radiometer for Nimbus 5, Proc. Roy. Soc. London, A334, 149-170, 1973.

Fleming, E. L., S. Chandra, J. J. Barnett, and M. Corney, Zonal mean temperature, Pressure, zonal wind and geopotential height as functions of latitude, Adv. Space. Res., 10, 11-59, 1990.

Forbes, J. M. and D. F. Gillette, A compendium of theoretical atmospheric tidal structures, Part 1: Model description and explicit structures due to realistic thermal and gravitational excitation, Project 6690, AFGL-TR-82-0173, Air Force Geophys. Lab, Bedford, Mass., 1982.

Garcia, R. R. and R. T. Clancy, Seasonal variation in equatorial mesospheric temperatures observed by SME, J. Atmos. Sci., 47, 1666-1673, 1990.

Gille, S. T., A. Hauchecorne, and M. L. Chanin, Semidiurnal and diurnal tidal effects in the middle atmosphere as seen by Rayleigh lidar, J. Geophys. Res., 96, 7579-7587, 1991.

Hauchecorne, A., M. L. Chanin, and R. Wilson, Mesospheric temperature inversion and gravity wave breaking, Geophys. Res. Lett., 14, 933-936, 1987.

Hedin, A. E., A revised thermospheric model based on mass spectrometer and incoherent scatter data, MSIS-83, J. Geophys. Res., 88, 10170-10185, 1983.

Lubken, F.- J. and U. von Zahn, Thermal structure of the mesopause region at polar latitudes, J. Geophys. Res., 96, 20841-20857, 1991.

Meriwether, J. W., P. D. Dao, R. T. McNutt, W. Klemetti, W. Moskowitz, and G. Davidson, Rayleigh lidar observations of mesosphere temperature structure, submitted to J. Geophys. Res., 1993.

Mount, G. H., D. W. Rusch, J. F. Noxon, J. M. Zawodny, and C. A. Barth, Measurements of stratospheric NO_2 from the Solar Mesosphere Explorer. 1. An overview of the results, J. Geophys. Res., 89, 1327-1340, 1984.

Rusch, D. W., G. H. Mount, C. A. Barth, R. J. Thomas, and M. T. Callan, Solar Mesosphere Explorer ultraviolet spectrometer: Measurements of ozone in the 1.0- to 0.1-mbar region, J. Geophys. Res., 89, 11677-11687, 1984.

Schmidlin, F. J., Temperature inversions near 75 km, Geophys. Res. Lett., 3, 173-176, 1976.

Schmidlin, F. J., H. S. Lee, and W. Michel, The inflatable sphere: A technique for the accurate measurement of middle atmosphere temperatures, J. Geophys. Res., 96, 22673-22682, 1991.

She, C. Y., J. R. Yu, and H. Chen, Observed thermal structure of a midlatitude mesopause, Geophys. Res. Lett., 20, 567-570, 1993.

Thomas, G. E., Solar Mesosphere Explorer measurements of polar mesospheric clouds (noctilucent clouds), J. Atmos. Terr. Phys., 46, 819-824, 1984.

Thomas, G. E., B. M. Jakosky, R. A. West, and R. W. Sanders, Satellite limb-scanning thermal infrared observations of the El Chichon stratospheric aerosol: First results, Geophys. Res. Lett., 10, 10997-11000, 1983.

Figure Captions

Figure 1. SME limb radiance profiles observed at 296 nm, 304 nm,313 nm, and 442 nm. The exponential portions of the profiles indicate the exponential decrease of the Rayleigh scattering atmosphere with altitude. The lower altitude maxima in the profiles indicate ozone absorption at the 296-313 nm wavelengths, and molecular/aerosol extinction at 442 nm.

Figure 2. Longitudinal coverages (at the equator) of the SME limb radiance profiles versus time over the 1982-1986 period. The 296 nm observations (G.P. 158) span the full period, whereas the 304/313 nm observations (G.P. 176, 195) began in 1983. The 442 nm observations were obtained at longitudes included in both panels. The latitudinal dependence of the zonal coverage is not large except at high latitudes, due to the near-polar, sun-synchronous orbit of SME.

Figure 3. Profiles of SME (dashed lines and symbols) and CIRA 86 monthly averaged temperatures for the upper stratosphere and mesosphere at 40°S latitude for the months of (a) January, (b) April, (c) July and (d) October The SME temperatures are obtained from 296 nm (diamond symbols), 304 nm (plus symbols), 313 nm (asterisk symbols), and 442 nm (triangle symbols) radiance profile measurements between 1982 and 1986. The dashed lines indicate a spline-smoothed fit over the 40-92 km altitude region to these individual temperature profile measurements, which were obtained for smaller altitude ranges. The CIRA 86 temperatures reflect 1973-1978 IR measurements below 80 km and the MSIS 83 model above 86 km.

Figure 4. Same as for figure 3, for 15°S latitude.

Figure 5. Same as for figure 3, for 0° latitude.

Figure 6. Same as for figure 3, for 15°N latitude.

Figure 7. Same as for figure 3, for 40°N latitude.

Figure 8. Comparisons of SME (dashed lines) and CIRA 86 (solid lines) temperature climatologies to datasonde rocket measurements (asterisk symbols) in 1982. The datasonde profiles reflect the averages of 8-29 separate rocket measurements for Ascension Island in (a) January and (b) March; (c) Barking Sands, HI in March; Pt. Mugu, CA in (d) January and (e) March; and (f) Wallops Island, VA in March. The error bars presented with the rocket profiles indicate the 1σ limits in the *distribution* of temperatures among the 8-29 observations reflected in the average rocket profiles. The average local time and number of rocket profiles for each average datasonde temperature profile are indicated for each comparison.

Figure 9. Comparisons of SME (dashed lines) and Haute Provence lidar temperature profiles, for the months of (a) January (b) March (c) May (d) July (e) September and (f) November. The 44°N lidar profiles are separated as averages obtained from 1981-1984 (dotted lines, Chanin et al., 1985) and 1981-1987 (solid lines, Chanin et al., 1990).

Figure 10. The January-to-June dependence of monthly average temperatures at 40°N for altitudes of (a) 85 km and (b) 90 km. The solid lines reflect linear fits to Urbana lidar nighttime observations in 1991 (Bills and Gardner, 1993); the plus symbols present the 2 pm SME climatology, and the asterisk symbols present the CIRA 86 climatological temperatures.

Figure 11. Comparisons of high latitude temperatures from the SME (dashed lines) and CIRA 86 (solid lines) climatologies, and monthly averages from Andenes, Norway (Lubken and von Zahn, 1991). SME profiles for (a) 70°N in March (b) 65°N in August and (c) 70°N in October are available for comparison to the 69°N location of Andenes, Norway. The Norway profiles incorporate lidar and in situ measurements from 1980 to 1990.

Figure 12. The annual dependences of temperatures at altitudes of 75 km (solid lines) and 85 km (dashed lines), from the SME (heavy lines) and CIRA 86 (light lines) climatologies. Figure 12 a presents these temperatures averaged over the latitude range 5°S-5°N. Figure 12b presents these temperatures averaged over the latitude range 30°S-40°S. Periods during which distinct temperature minima are observed at altitudes of 70-80 km for the SME climatology are indicated by arrows on each figure.

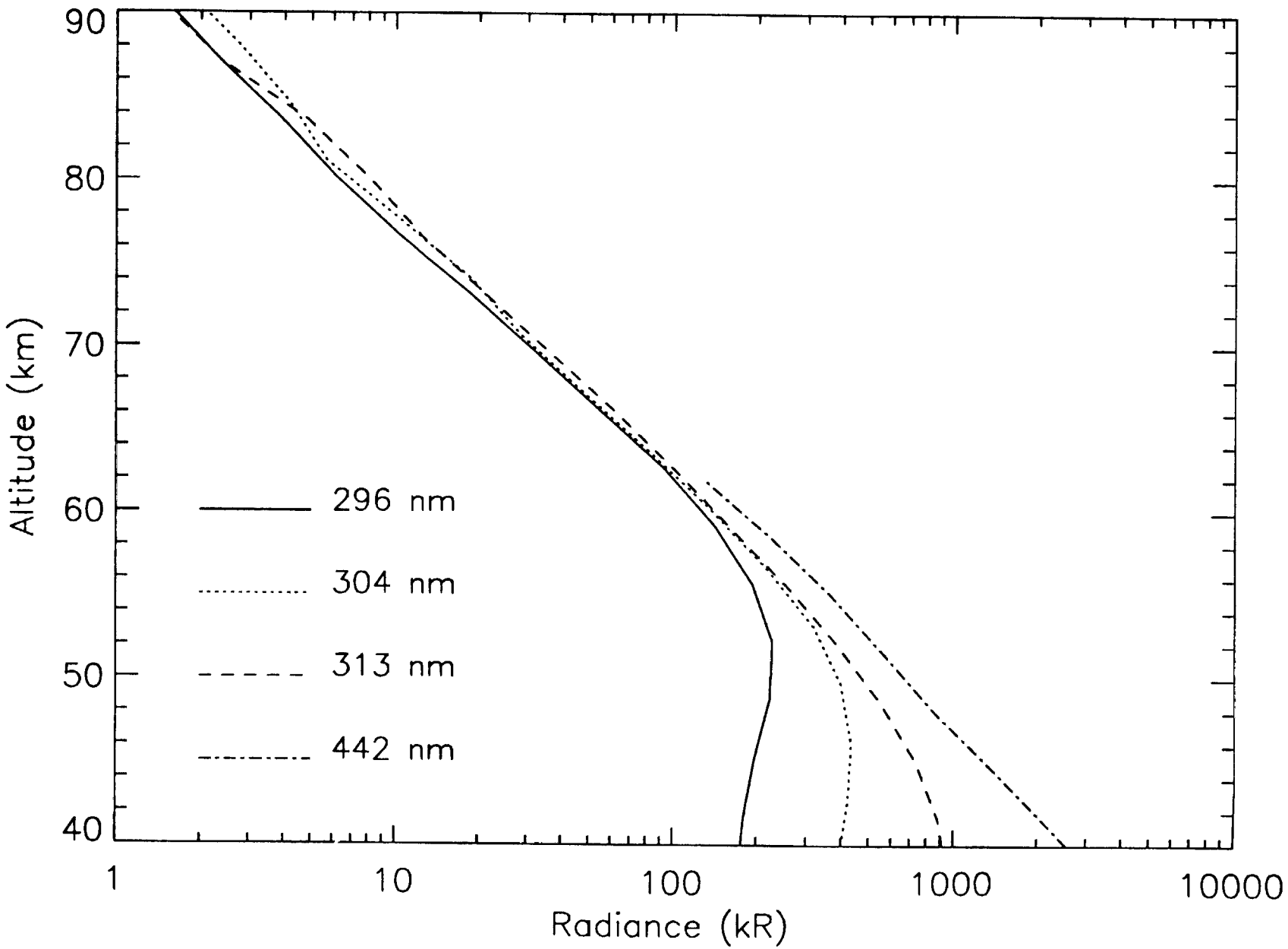
90
80
70
60
50
40
Altitude (km)
296 nm
304 nm
313 nm
442 nm
1
10
100
1000
10000
Radiance (kR)

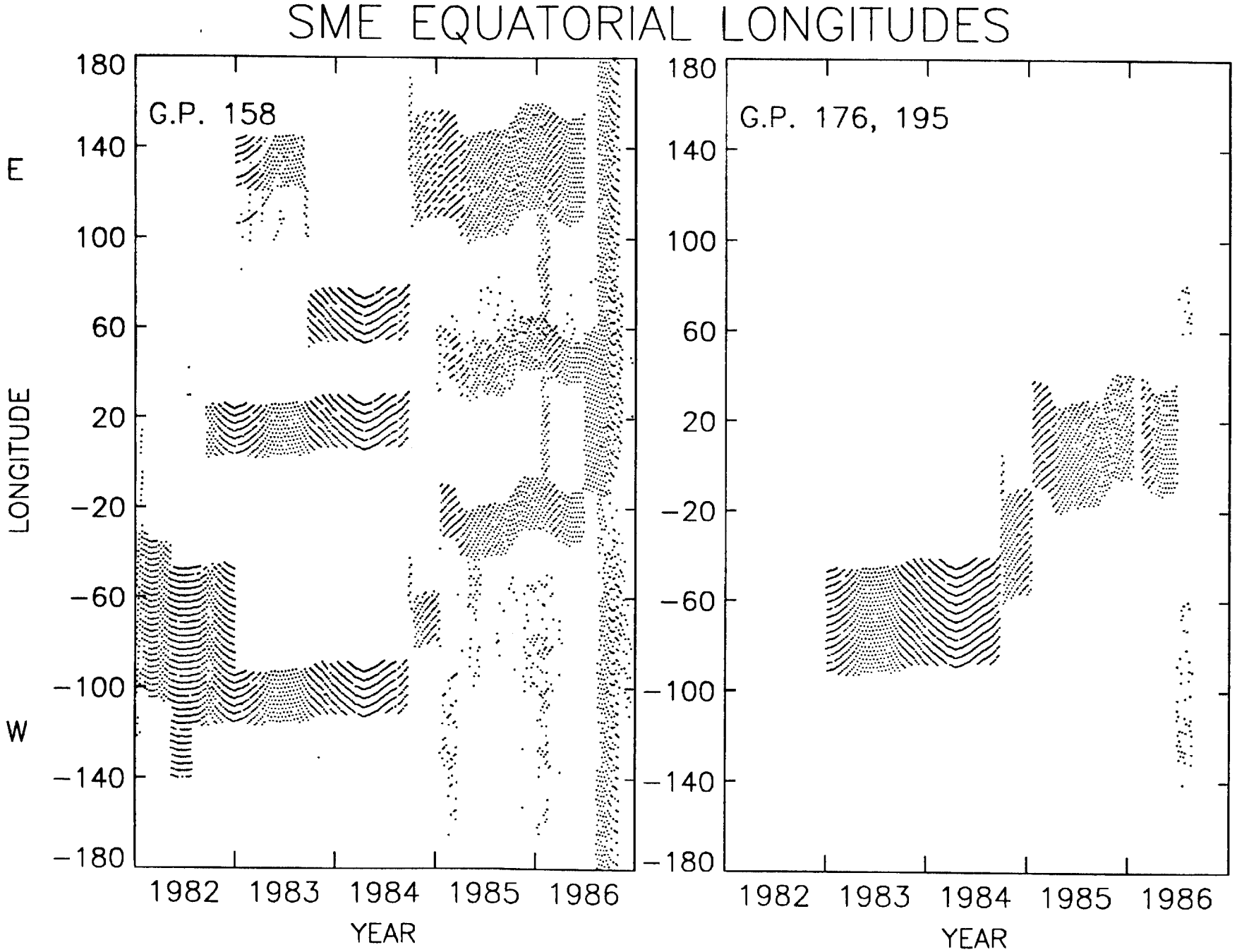
SME EQUATORIAL LONGITUDES
G.P. 158
G.P. 176, 195
LONGITUDE
E
W
180
140
100
60
20
−20
−60
−100
−140
−180
1982
1983
1984
1985
1986
YEAR

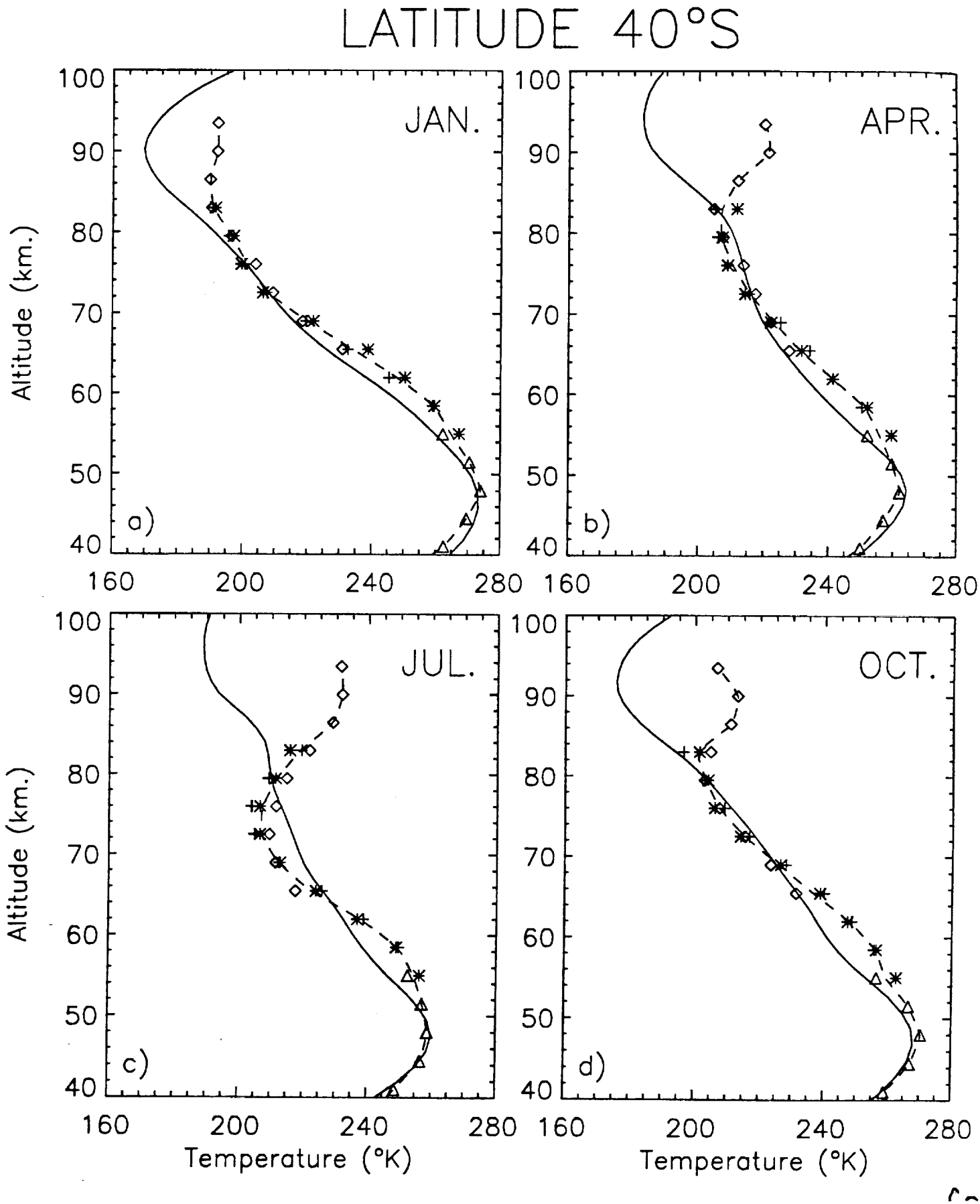
LATITUDE 40°S
JAN.
APR.
JUL.
OCT.
a)
b)
c)
d)
Altitude (km.)
Temperature (°K)
100
90
80
70
60
50
40
160
200
240
280

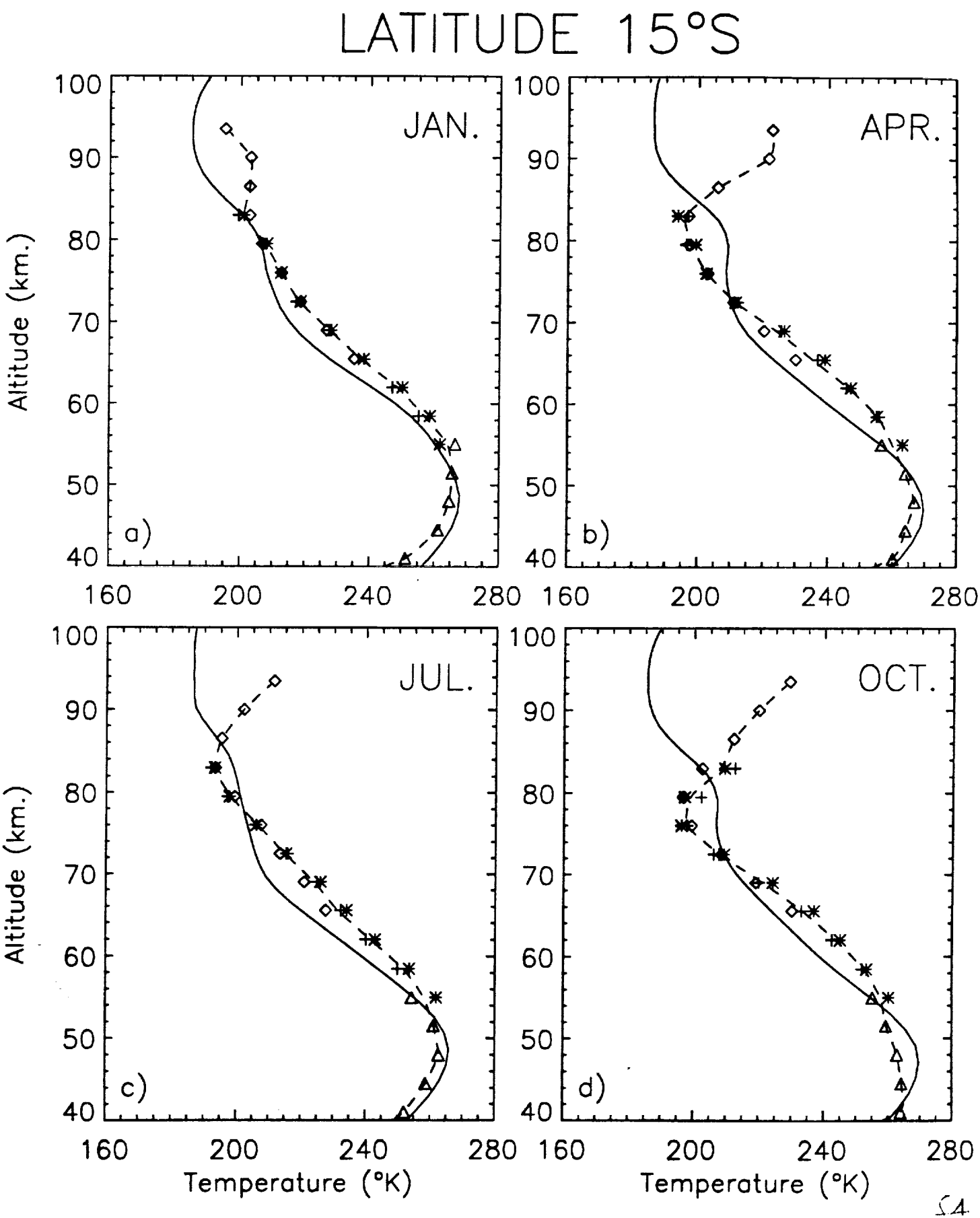
LATITUDE 15°S
JAN.
APR.
JUL.
OCT.
a)
b)
c)
d)
Altitude (km.)
Temperature (°K)
100
90
80
70
60
50
40
160
200
240
280

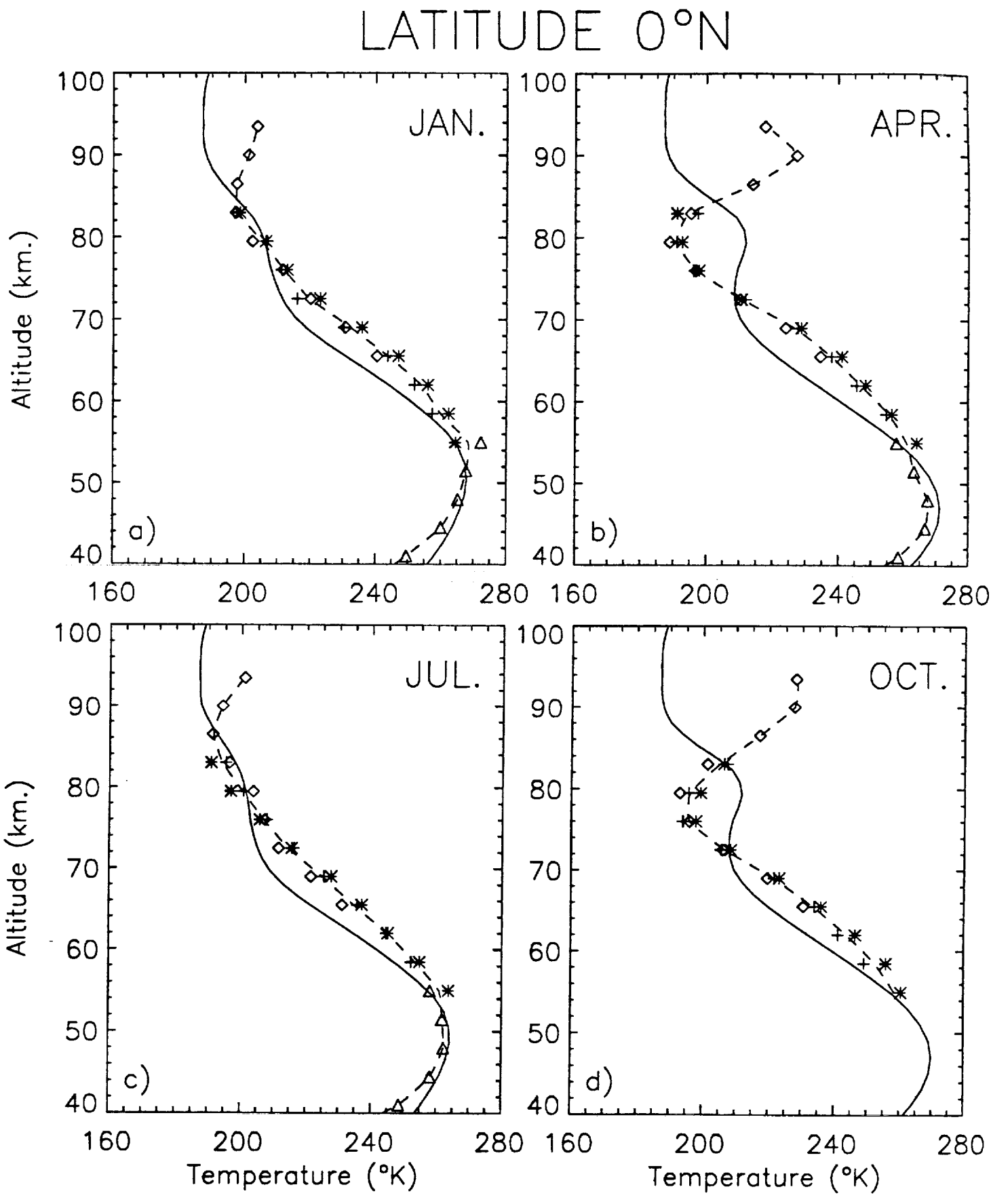
LATITUDE 0°N
JAN.
APR.
JUL.
OCT.
a)
b)
c)
d)
Altitude (km.)
Temperature (°K)
100
90
80
70
60
50
40
160
200
240
280

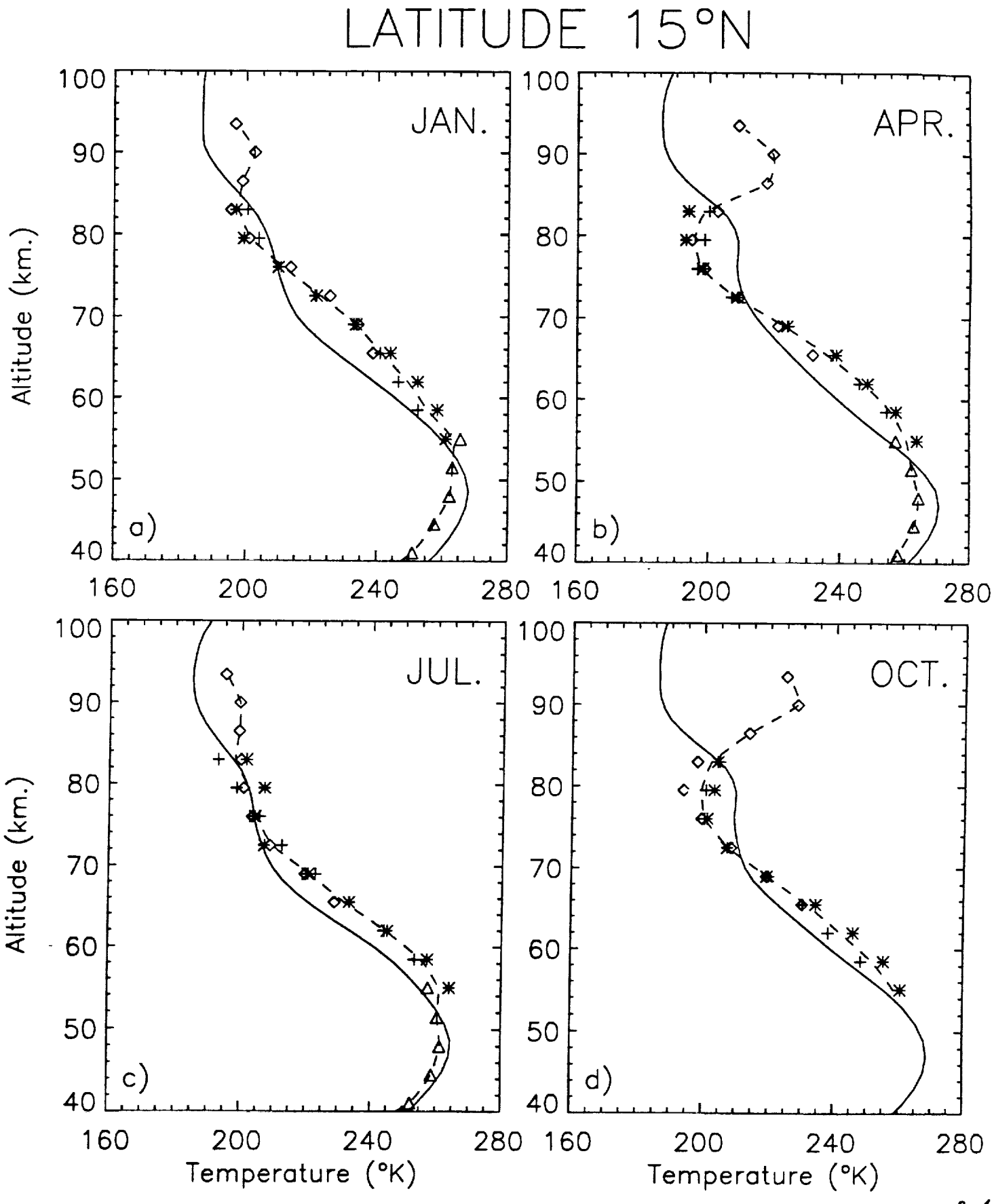
LATITUDE 15°N
JAN.
APR.
JUL.
OCT.
a)
b)
c)
d)
Altitude (km.)
Temperature (°K)
100
90
80
70
60
50
40
160
200
240
280

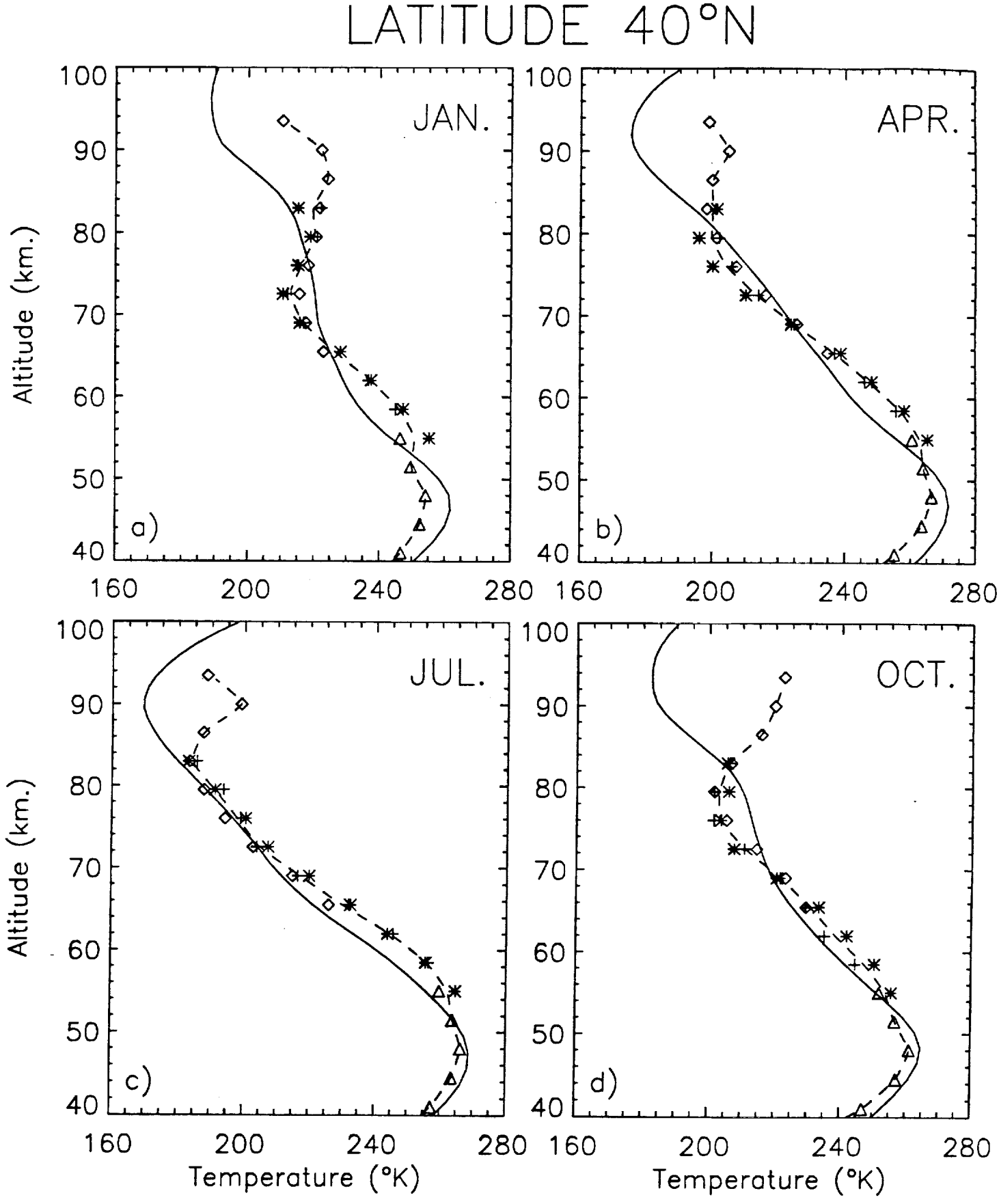
LATITUDE 40°N
JAN.
APR.
JUL.
OCT.
a)
b)
c)
d)
Altitude (km.)
Temperature (°K)
100
90
80
70
60
50
40
160
200
240
280

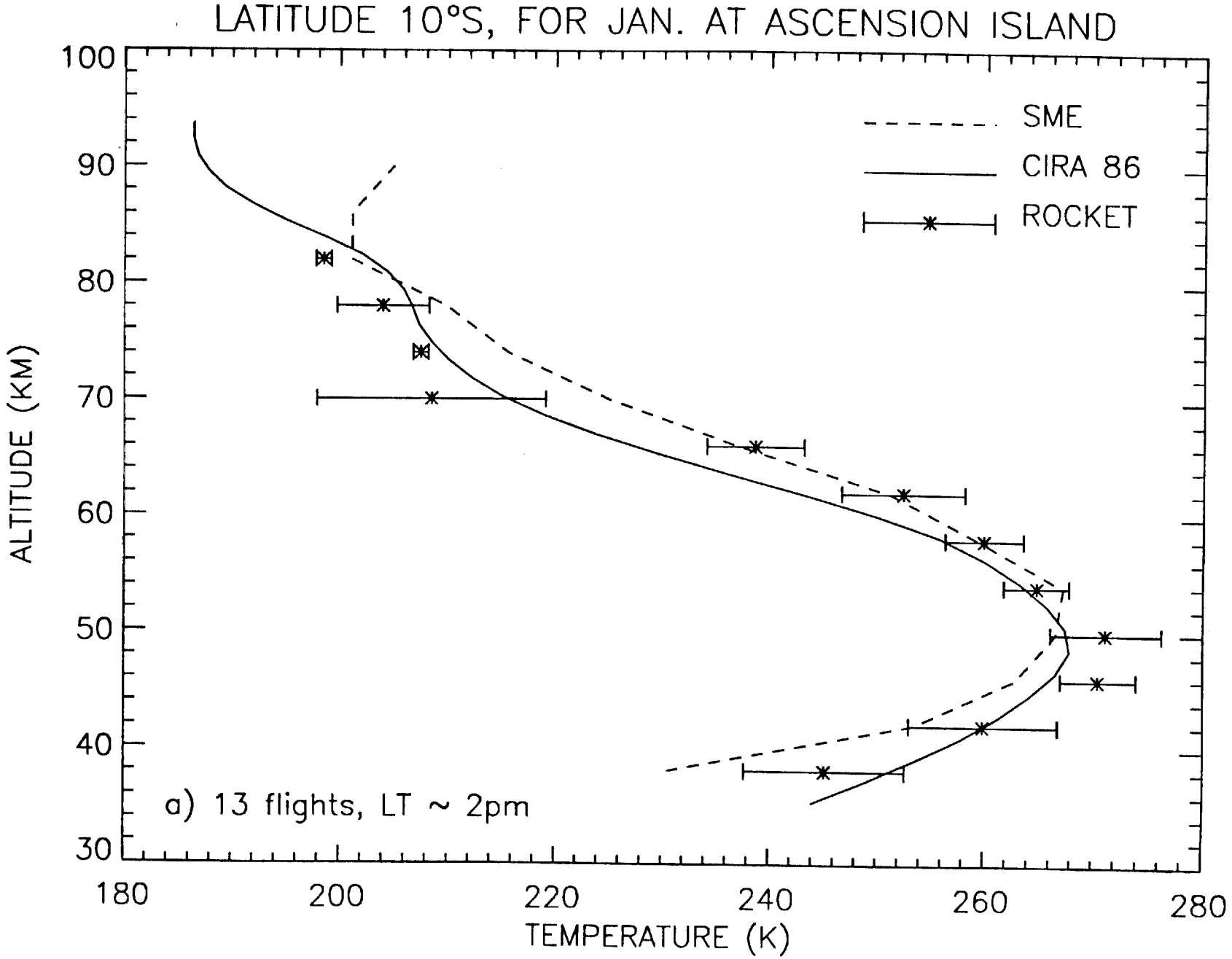
LATITUDE 10°S, FOR JAN. AT ASCENSION ISLAND
SME
CIRA 86
ROCKET
a) 13 flights, LT ~ 2pm
ALTITUDE (KM)
TEMPERATURE (K)
100
90
80
70
60
50
40
30
180
200
220
240
260
280

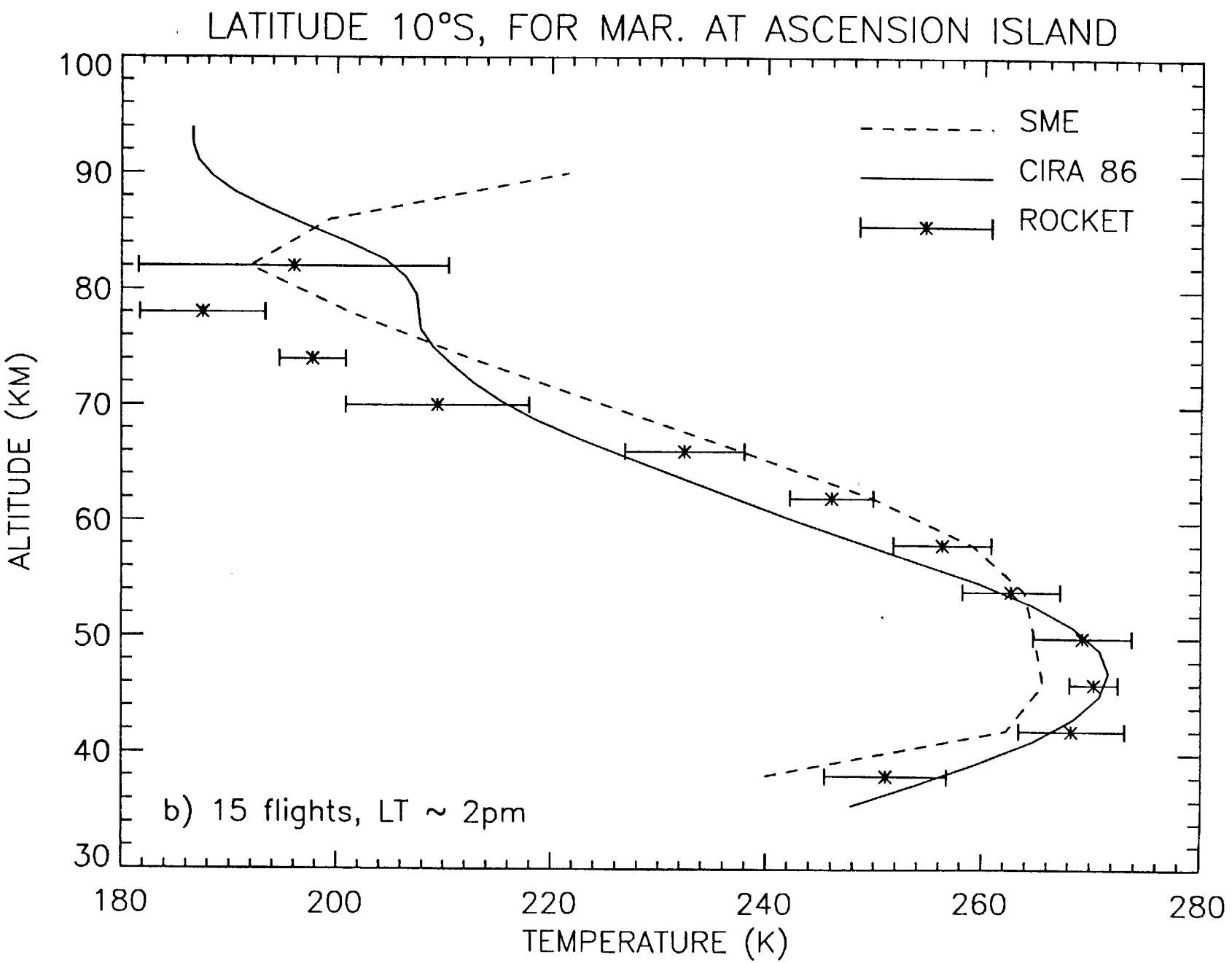
LATITUDE 10°S, FOR MAR. AT ASCENSION ISLAND
SME
CIRA 86
ROCKET
b) 15 flights, LT ~ 2pm
ALTITUDE (KM)
TEMPERATURE (K)
100
90
80
70
60
50
40
30
180
200
220
240
260
280

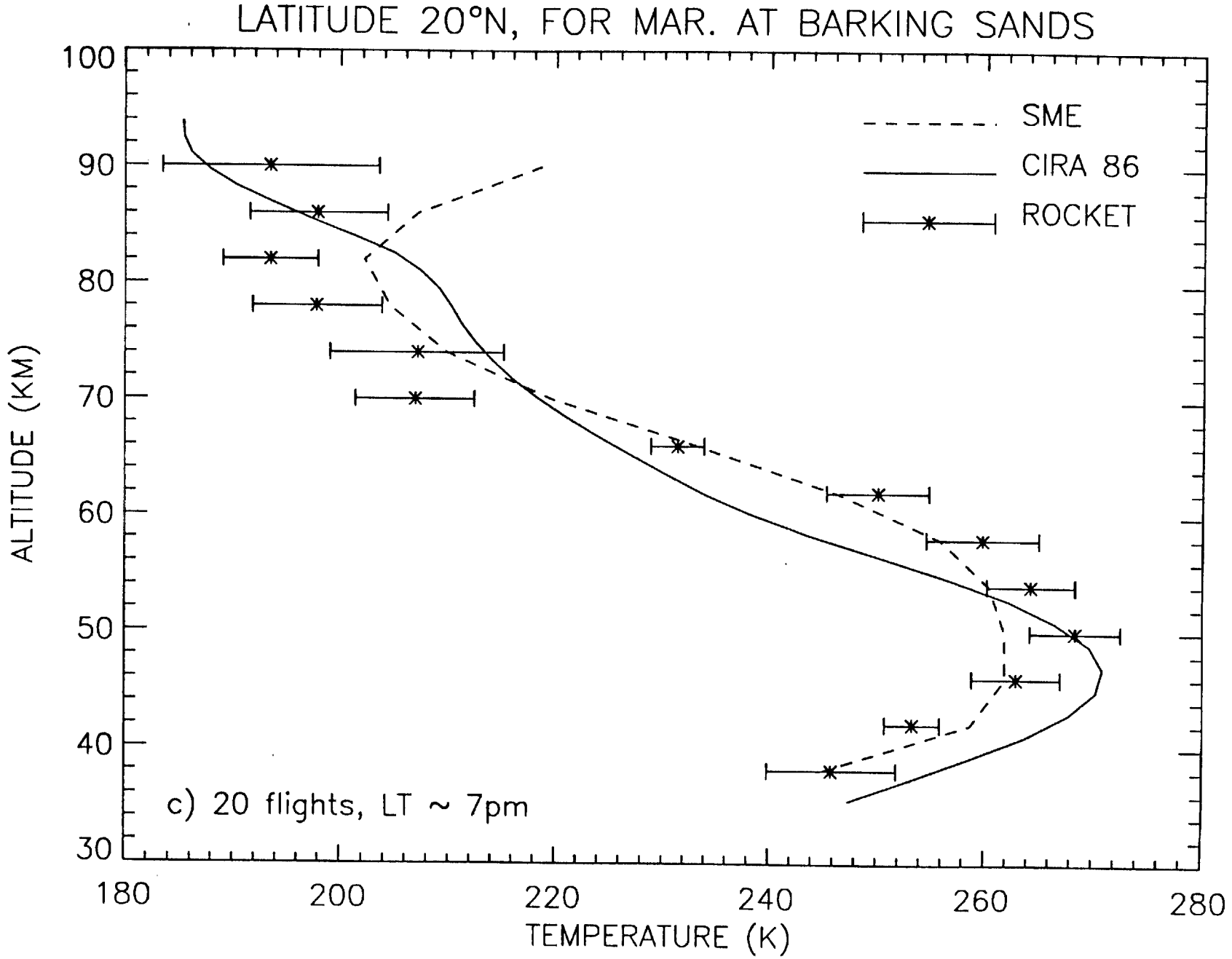
LATITUDE 20°N, FOR MAR. AT BARKING SANDS
SME
CIRA 86
ROCKET
c) 20 flights, LT ~ 7pm
ALTITUDE (KM)
TEMPERATURE (K)
100
90
80
70
60
50
40
30
180
200
220
240
260
280

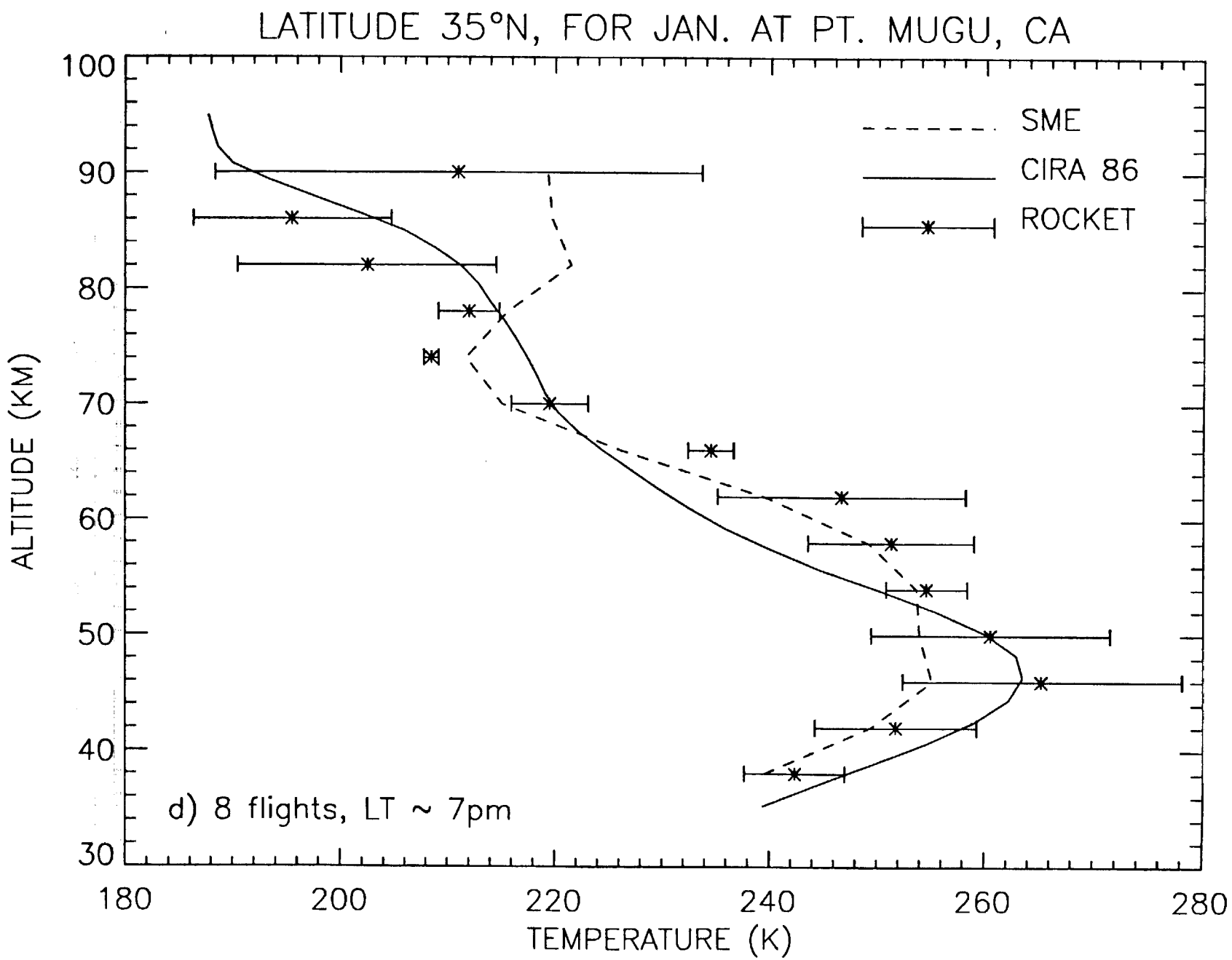
LATITUDE 35°N, FOR JAN. AT PT. MUGU, CA
SME
CIRA 86
ROCKET
d) 8 flights, LT ~ 7pm
ALTITUDE (KM)
TEMPERATURE (K)
100
90
80
70
60
50
40
30
180
200
220
240
260
280

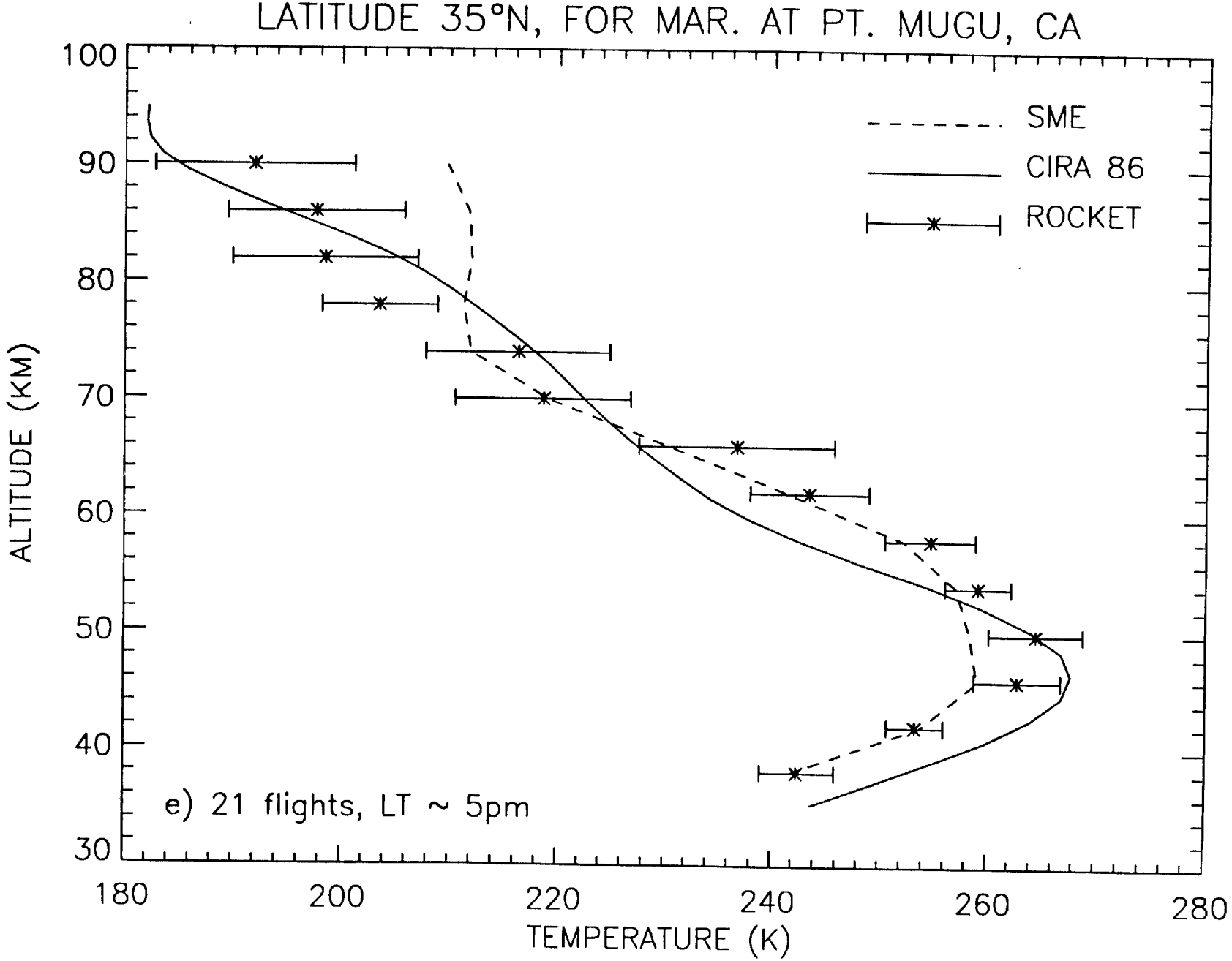
LATITUDE 35°N, FOR MAR. AT PT. MUGU, CA
SME
CIRA 86
ROCKET
e) 21 flights, LT ~ 5pm
ALTITUDE (KM)
TEMPERATURE (K)
100
90
80
70
60
50
40
30
180
200
220
240
260
280

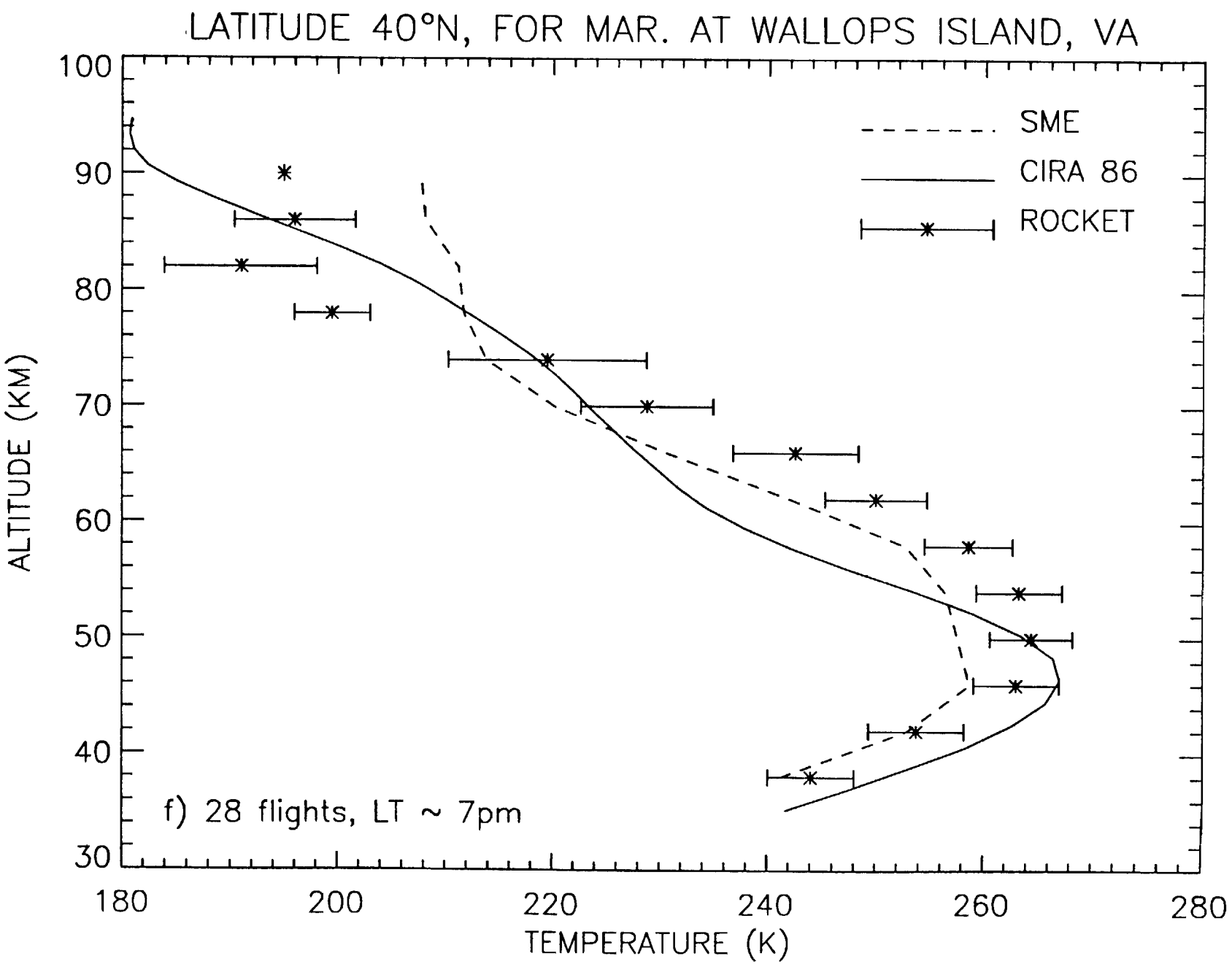
LATITUDE 40°N, FOR MAR. AT WALLOPS ISLAND, VA
SME
CIRA 86
ROCKET
f) 28 flights, LT ~ 7pm
ALTITUDE (KM)
TEMPERATURE (K)
100
90
80
70
60
50
40
30
180
200
220
240
260
280

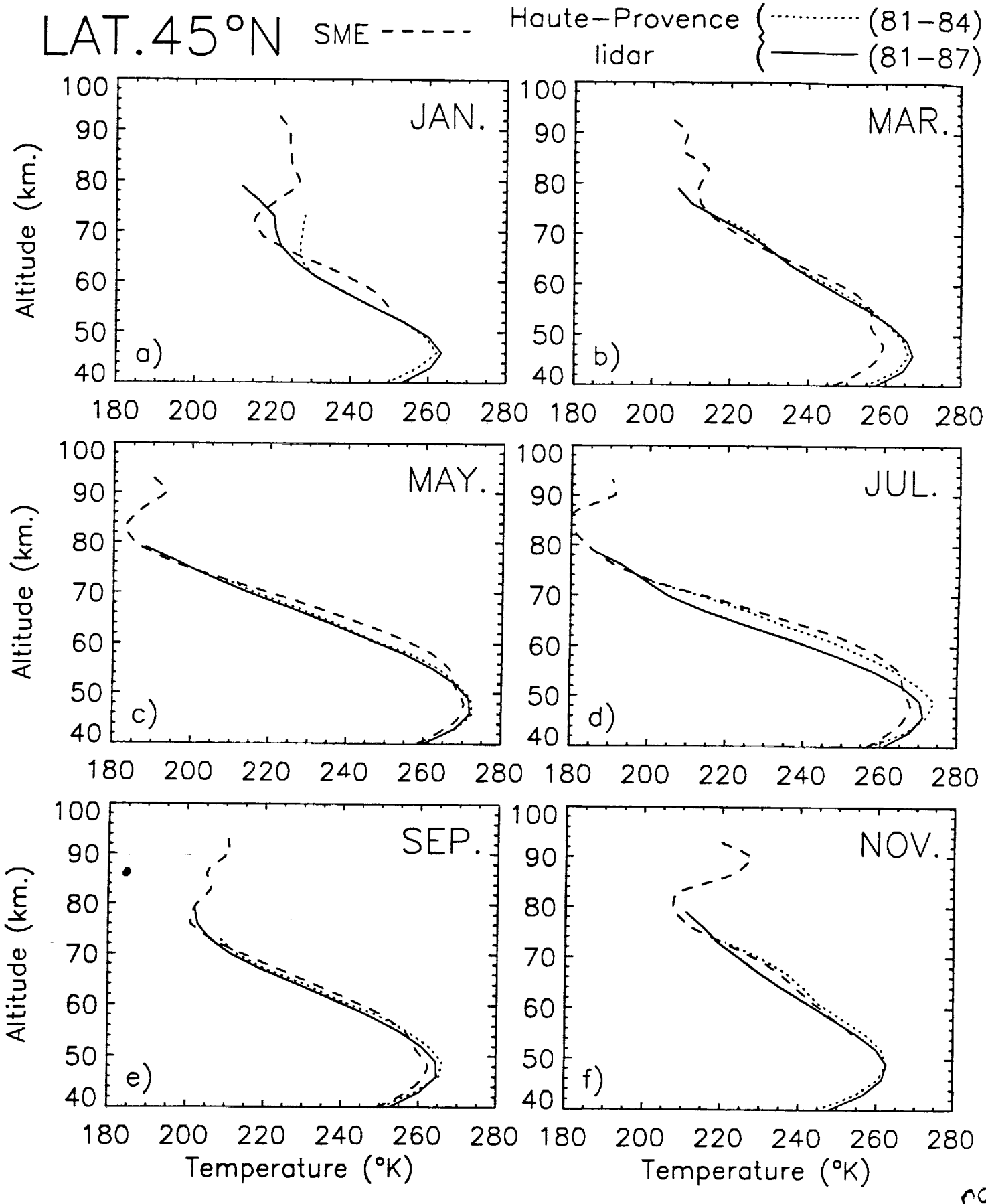
LAT.45°N
SME -----
Haute-Provence lidar
(81-84)
(81-87)
JAN.
MAR.
MAY.
JUL.
SEP.
NOV.
a)
b)
c)
d)
e)
f)
Altitude (km.)
Temperature (°K)
100
90
80
70
60
50
40
180
200
220
240
260
280

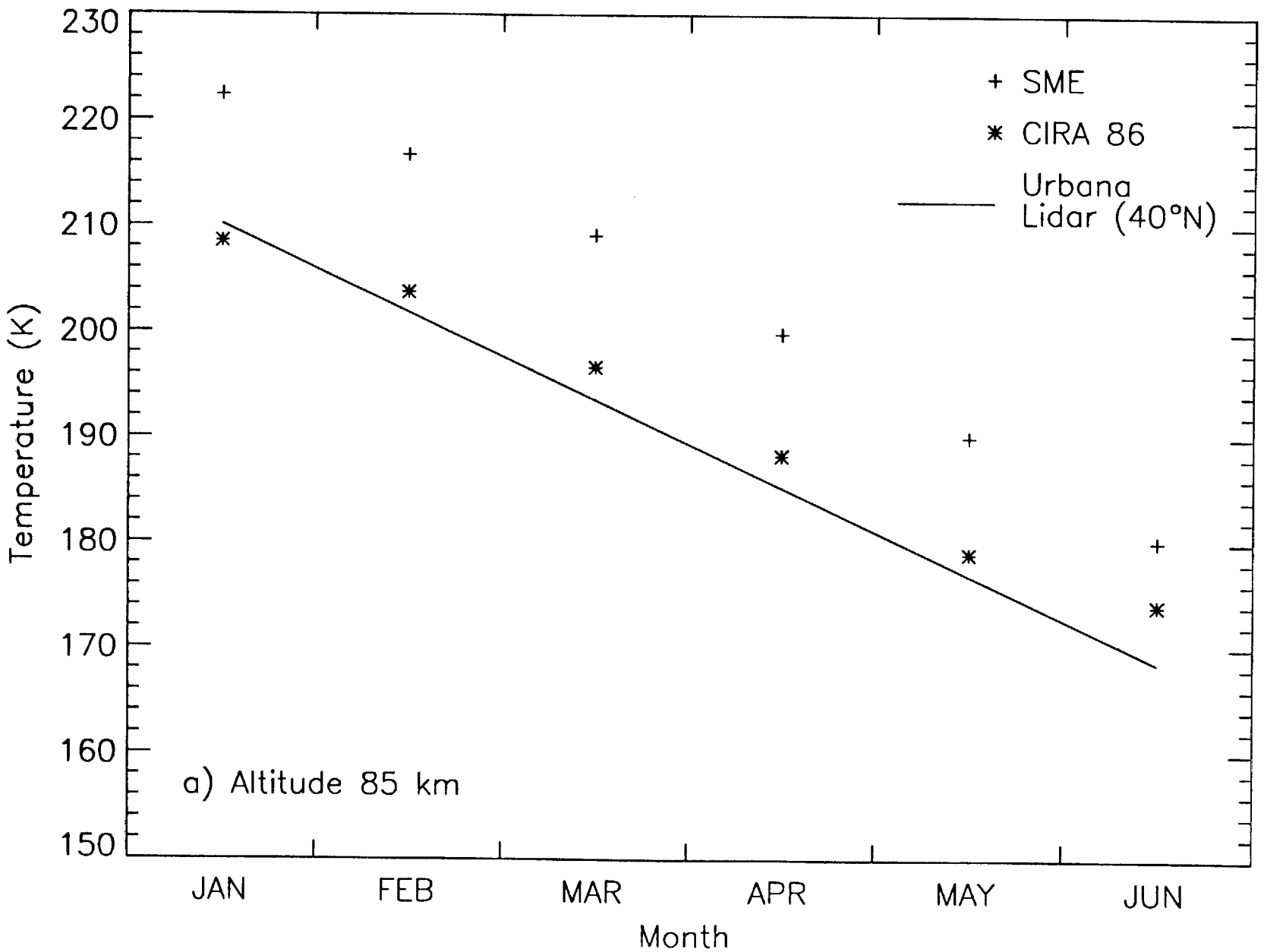
230
220
210
200
190
180
170
160
150
Temperature (K)
JAN
FEB
MAR
APR
MAY
JUN
Month
+ SME
* CIRA 86
Urbana Lidar (40°N)
a) Altitude 85 km

fig 10a

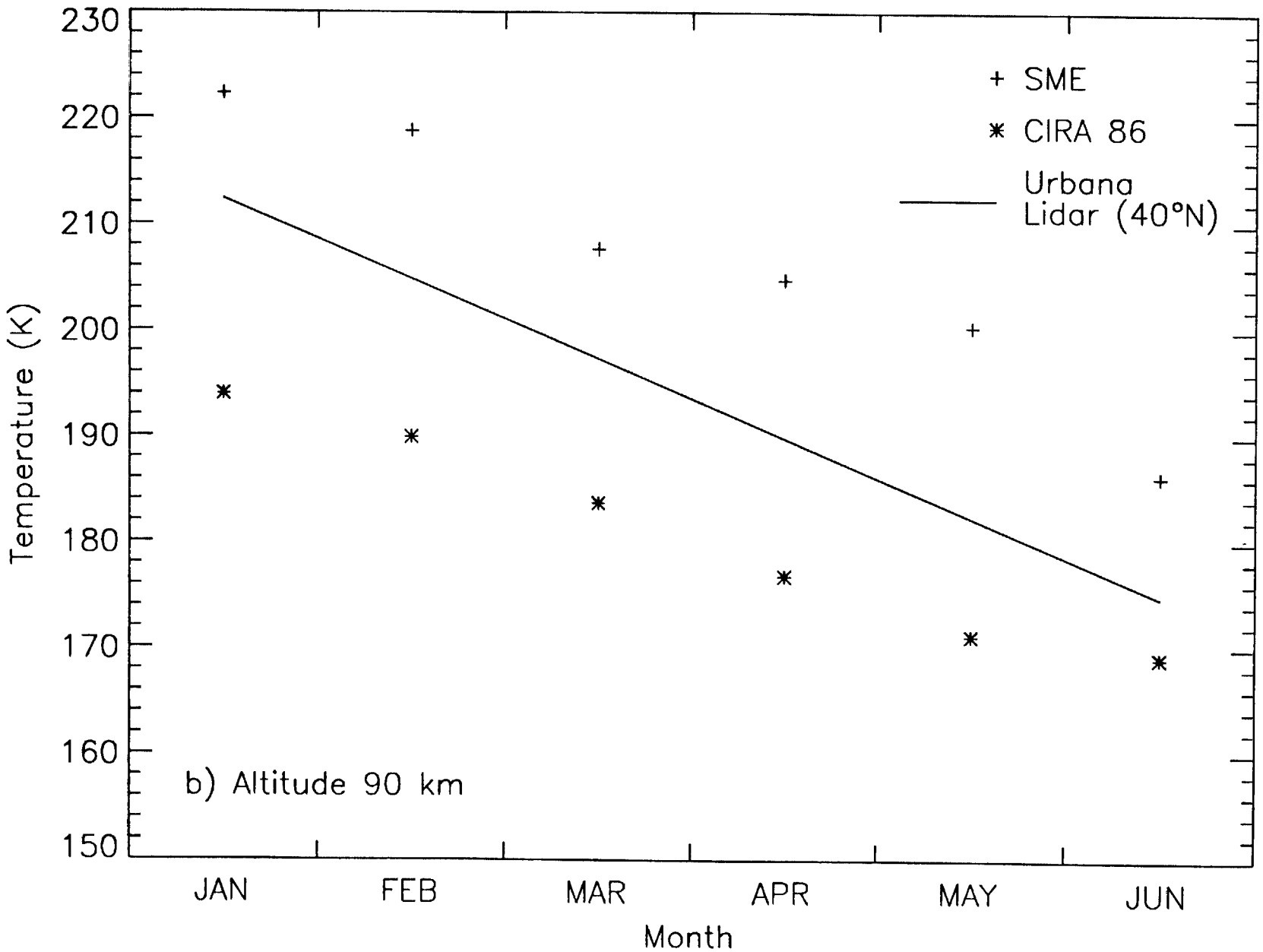
230
220
210
200
190
180
170
160
150
Temperature (K)
JAN
FEB
MAR
APR
MAY
JUN
Month
+ SME
* CIRA 86
Urbana
Lidar (40°N)
b) Altitude 90 km

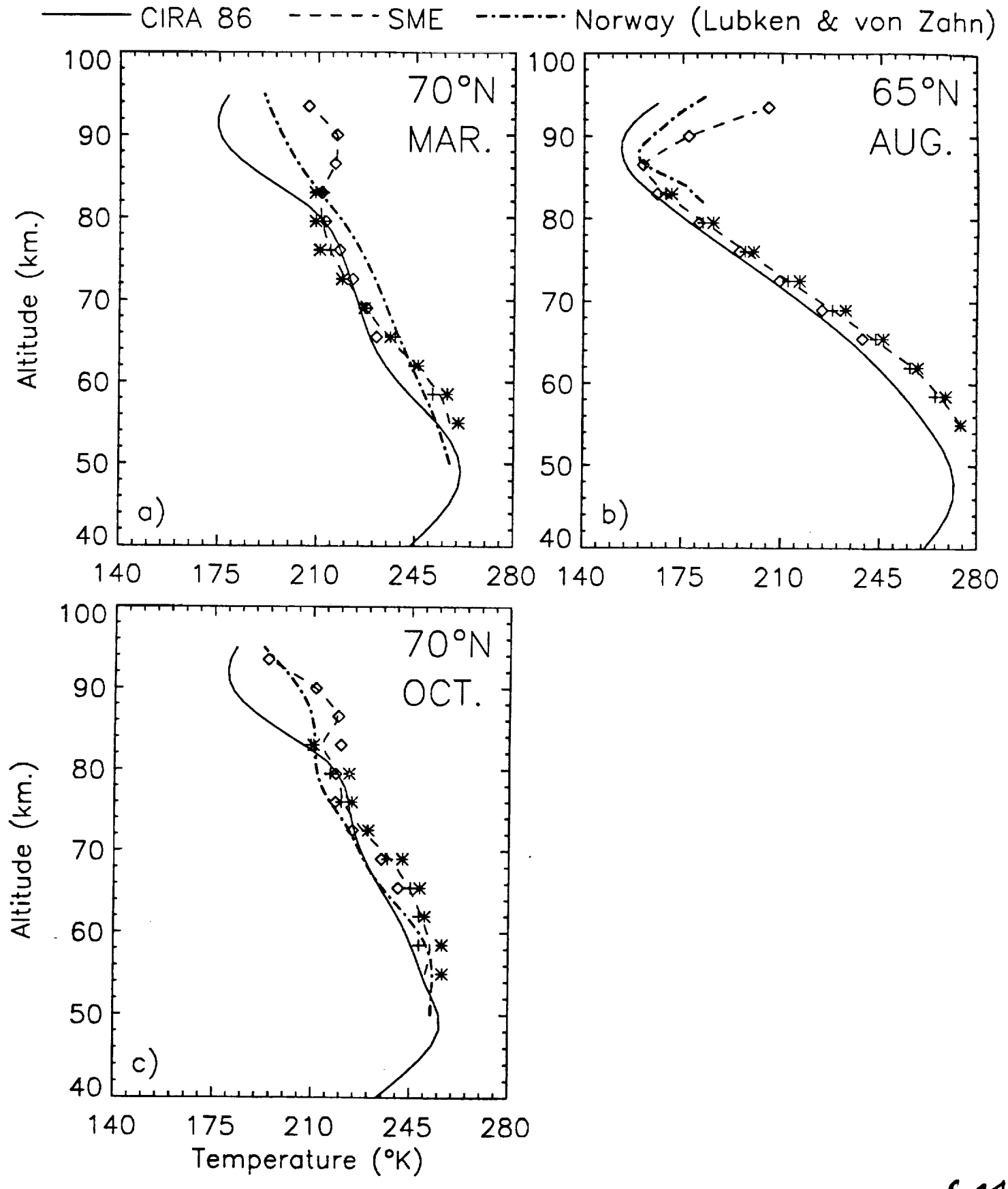
CIRA 86
SME
Norway (Lubken & von Zahn)
70°N
MAR.
a)
65°N
AUG.
b)
70°N
OCT.
c)
Altitude (km.)
Temperature (°K)
100
90
80
70
60
50
40
140
175
210
245
280

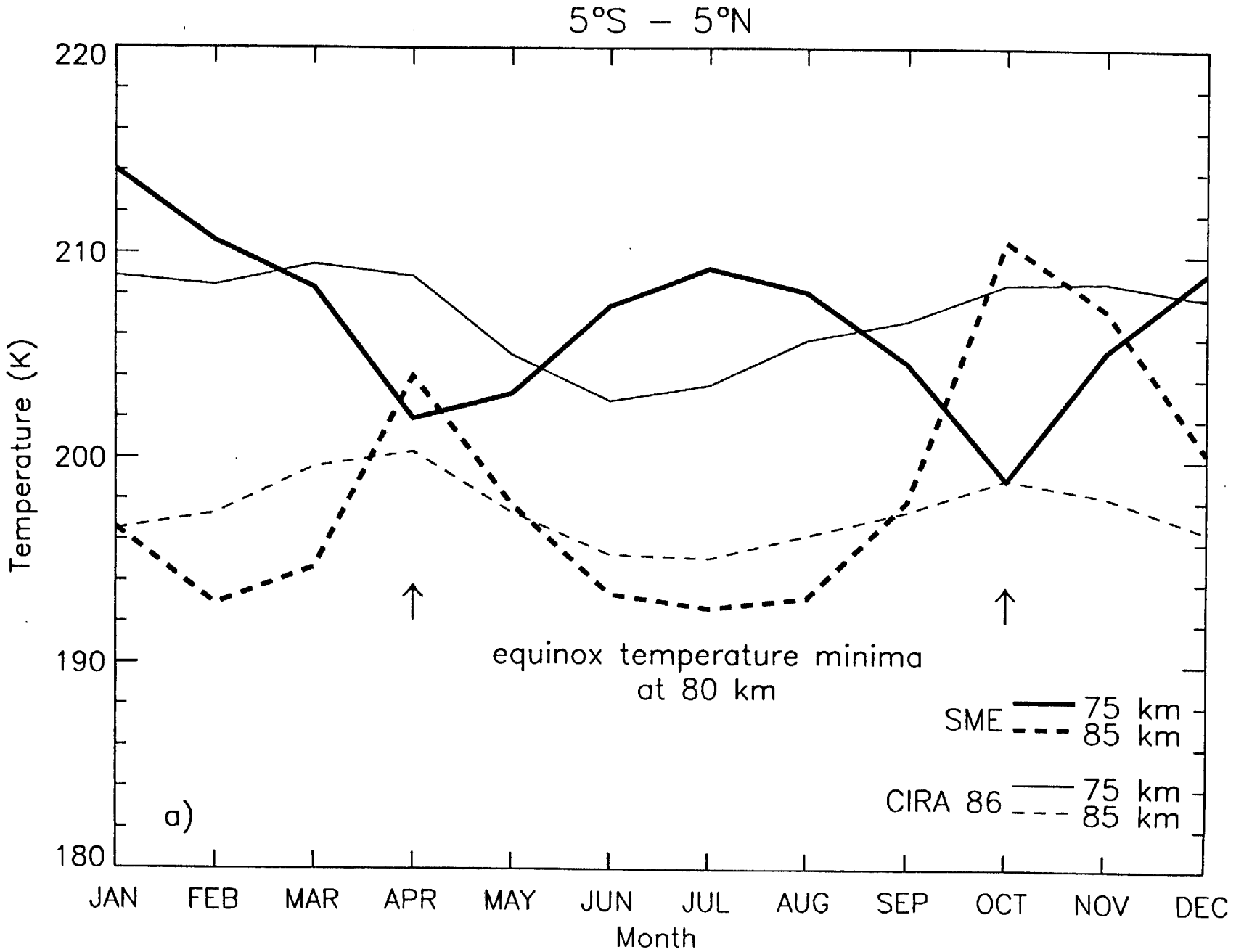
5°S – 5°N
220
210
200
190
180
Temperature (K)
JAN
FEB
MAR
APR
MAY
JUN
JUL
AUG
SEP
OCT
NOV
DEC
Month
equinox temperature minima
at 80 km
SME 75 km
85 km
CIRA 86 75 km
85 km
a)

f12a

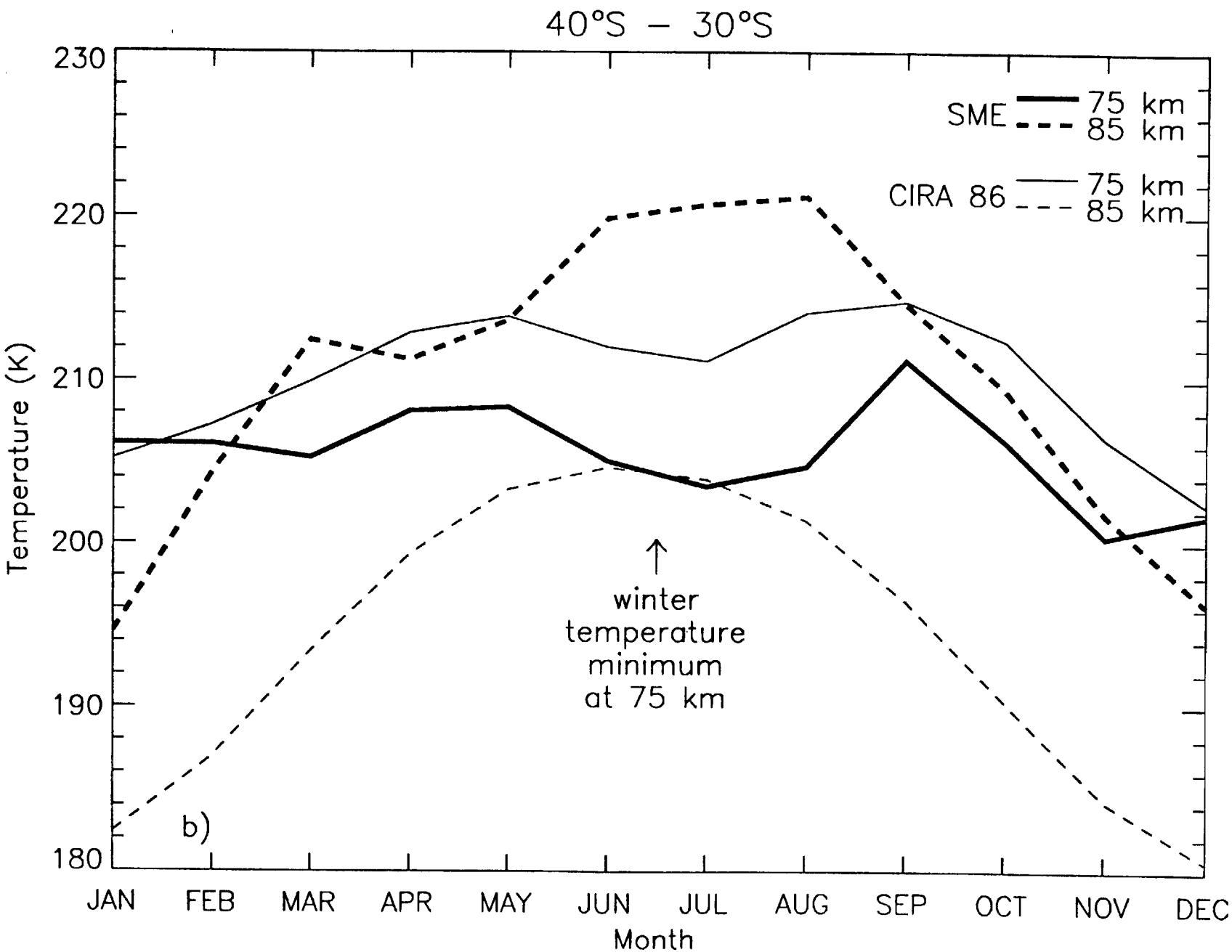
40°S – 30°S
230
220
210
200
190
180
Temperature (K)
SME 75 km
85 km
CIRA 86 75 km
85 km
winter
temperature
minimum
at 75 km
b)
JAN
FEB
MAR
APR
MAY
JUN
JUL
AUG
SEP
OCT
NOV
DEC
Month

APPENDIX A: SME TEMPERATURE CLIMATOLOGY

JANUARY

SOUTH LATITUDE

ALT.	75	70	65	60	55	50	45	40	35	30	25	20	15	10	5	0
40	0	0	0	0	0	263	261	259	256	253	250	247	245	244	245	246
44	0	0	0	0	0	273	271	269	266	265	263	260	260	259	259	259
48	0	0	0	0	0	280	277	274	271	269	267	265	265	265	265	265
52	0	0	0	0	0	276	273	270	267	265	264	264	266	267	268	268
56	0	0	0	0	276	269	267	263	262	260	258	260	262	265	266	266
60	0	0	0	0	266	262	257	255	251	248	247	250	253	255	257	257
64	0	0	0	0	253	248	243	240	237	235	235	239	242	244	247	248
68	0	0	0	0	238	231	228	224	224	225	226	229	230	231	234	236
72	0	0	0	0	223	213	211	209	212	214	218	218	219	219	222	221
76	0	0	0	0	197	197	198	202	205	208	213	212	213	213	214	212
80	0	0	0	0	177	187	190	196	202	202	206	209	207	206	204	204
84	0	0	0	0	173	178	185	190	198	198	202	203	201	199	198	197
88	0	0	0	0	167	178	185	191	195	195	204	202	203	203	202	199
92	0	0	0	0	177	183	186	192	190	198	196	203	199	205	202	203

NORTH LATITUDE

ALT	0	5	10	15	20	25	30	35	40	45	50	55	60	65	70	75
40	246	245	247	248	248	246	246	245	244	0	0	0	0	0	0	0
44	259	257	257	257	256	256	254	253	252	0	0	0	0	0	0	0
48	265	265	264	262	260	260	258	256	254	0	0	0	0	0	0	0
52	268	268	267	263	260	258	255	252	250	0	0	0	0	0	0	0
56	266	265	264	261	258	256	254	253	250	249	248	247	0	0	0	0
60	257	257	255	253	250	247	245	245	242	242	241	242	0	0	0	0
64	248	249	246	245	242	238	236	233	231	230	232	237	0	0	0	0
68	236	237	237	236	233	229	226	220	219	220	225	232	0	0	0	0
72	221	223	224	224	221	219	217	212	213	215	221	225	0	0	0	0
76	212	209	211	211	210	212	212	213	216	221	223	219	0	0	0	0
80	204	198	200	201	204	206	207	219	220	227	226	219	0	0	0	0
84	197	193	194	198	203	207	208	222	221	225	227	221	0	0	0	0
88	199	197	195	201	202	210	212	219	224	224	229	225	0	0	0	0
92	203	205	204	200	197	200	208	215	216	222	219	225	0	0	0	0

FEBRUARY

SOUTH LATITUDE

ALT.	75	70	65	60	55	50	45	40	35	30	25	20	15	10	5	0
40	0	0	0	0	0	260	259	257	255	253	251	248	0	0	248	249
44	0	0	0	0	0	269	269	267	265	264	263	262	0	0	263	263
48	0	0	0	0	0	275	274	272	269	267	265	265	0	0	267	267
52	0	0	0	0	0	271	268	267	264	263	261	262	0	0	266	266
56	0	0	273	272	270	264	261	259	258	258	259	261	264	264	265	265
60	0	0	265	262	259	257	253	250	248	248	251	254	256	257	258	257
64	0	0	252	249	245	241	238	236	235	235	238	242	243	245	246	248
68	0	0	235	234	229	225	224	223	223	225	227	228	229	231	233	235
72	0	0	216	211	211	209	209	210	211	215	215	214	215	218	219	220
76	0	0	199	191	195	196	198	202	204	208	208	206	208	208	207	207
80	0	0	183	182	186	188	192	199	204	207	206	205	205	201	197	199
84	0	0	170	176	183	188	194	199	205	208	204	204	201	199	192	194
88	0	0	170	181	189	195	200	201	206	205	206	205	205	208	204	204
92	0	0	190	194	197	200	198	202	200	195	205	206	207	210	220	217

NORTH LATITUDE

ALT	0	5	10	15	20	25	30	35	40	45	50	55	60	65	70	75
40	249	248	251	251	251	250	248	248	247	245	0	0	0	0	0	0
44	263	261	260	260	259	259	258	257	256	254	0	0	0	0	0	0
48	267	267	266	264	262	261	261	260	259	257	0	0	0	0	0	0
52	266	267	266	263	261	258	258	256	254	253	0	0	0	0	0	0
56	265	263	262	260	258	256	255	253	251	250	253	251	251	252	0	0
60	257	256	254	253	250	247	246	245	243	243	244	246	247	247	0	0
64	248	248	246	244	241	238	236	234	232	232	233	236	239	240	0	0
68	235	237	236	234	231	228	224	223	222	222	225	229	232	233	0	0
72	220	221	221	221	219	216	214	216	216	217	220	224	229	226	0	0
76	207	209	207	209	208	208	210	215	216	217	219	219	224	224	0	0
80	199	197	198	199	203	206	212	215	217	221	221	219	218	225	0	0
84	194	191	196	197	203	207	211	215	216	223	223	222	219	225	0	0
88	204	198	205	206	209	207	208	215	218	222	229	236	233	228	0	0
92	217	215	209	207	204	204	205	211	216	221	227	233	232	224	0	0

MARCH

SOUTH LATITUDE

ALT.	75	70	65	60	55	50	45	40	35	30	25	20	15	10	5	0
40	0	0	0	0	0	252	252	252	252	252	252	251	252	254	256	257
44	0	0	0	0	0	262	262	263	263	263	263	263	263	265	266	266
48	0	0	0	0	0	268	268	268	269	268	267	267	267	266	267	267
52	0	0	0	0	0	263	263	263	264	264	264	264	263	264	263	263
56	261	261	261	262	261	257	256	256	257	257	259	260	261	262	262	261
60	256	255	254	252	250	249	248	248	249	251	252	254	254	255	254	253
64	246	244	242	239	236	235	234	235	237	239	241	242	243	244	244	244
68	233	231	228	224	221	220	220	221	224	225	228	229	231	232	233	234
72	220	217	214	211	208	206	206	209	210	213	215	214	217	218	220	220
76	210	206	204	201	201	201	202	204	204	204	205	205	207	207	206	205
80	200	198	198	197	198	204	206	207	205	204	203	202	199	196	195	193
84	191	194	197	200	204	208	210	212	211	209	203	201	197	193	192	192
88	192	201	207	213	217	216	211	214	213	213	211	207	211	210	206	210
92	205	206	213	214	214	213	208	203	206	210	217	218	222	223	229	231

NORTH LATITUDE

ALT.	0	5	10	15	20	25	30	35	40	45	50	55	60	65	70	75
40	257	258	256	255	253	251	249	249	248	246	245	0	0	0	0	0
44	266	265	265	262	261	259	258	257	257	256	255	0	0	0	0	0
48	267	267	267	265	262	262	261	260	260	260	259	0	0	0	0	0
52	263	263	264	263	261	259	259	257	256	256	256	0	0	0	0	0
56	261	261	260	260	259	257	257	256	255	255	255	255	254	255	257	254
60	253	252	251	252	251	250	249	247	248	248	249	249	249	247	250	248
64	244	244	243	243	240	238	237	236	236	237	238	240	240	238	239	239
68	234	234	233	231	226	225	225	224	225	226	227	230	229	230	229	232
72	220	219	219	216	214	215	215	215	216	218	219	219	221	222	221	223
76	205	203	204	204	207	209	211	210	212	212	213	212	215	213	214	216
80	193	192	193	199	203	207	211	212	211	212	212	212	214	210	211	215
84	192	193	195	200	204	208	211	212	210	213	212	211	212	211	212	214
88	210	208	210	210	213	212	213	211	208	208	213	212	215	214	217	215
92	231	222	218	219	217	212	210	204	205	206	208	208	215	213	212	203

APRIL

SOUTH LATITUDE

ALT.	75	70	65	60	55	50	45	40	35	30	25	20	15	10	5	0
40	0	0	0	0	0	242	244	246	248	250	251	253	254	255	256	254
44	0	0	0	0	0	252	254	256	258	260	261	262	264	262	262	266
48	0	0	0	0	0	258	260	262	264	266	266	266	267	265	265	267
52	0	0	0	0	0	257	258	259	261	262	263	263	263	263	262	263
56	0	0	0	253	255	253	253	255	256	258	258	259	259	260	260	260
60	0	0	0	247	246	246	246	247	249	250	251	252	252	252	252	252
64	0	0	0	238	235	235	234	236	238	239	239	240	240	240	241	242
68	0	0	0	233	228	226	226	226	226	227	226	226	227	229	229	230
72	0	0	0	228	224	222	220	217	215	214	213	214	213	215	215	213
76	0	0	0	223	221	219	215	211	205	203	203	204	203	202	201	197
80	0	0	0	220	216	217	210	207	202	198	198	197	197	193	192	191
84	0	0	0	217	213	214	210	208	209	207	204	202	198	199	197	200
88	0	0	0	221	218	216	216	216	218	221	220	215	213	216	215	220
92	0	0	0	216	219	218	219	221	216	219	218	213	223	218	222	223

NORTH LATITUDE

ALT.	0	5	10	15	20	25	30	35	40	45	50	55	60	65	70	75
40	254	256	256	256	254	253	252	252	252	252	252	0	0	0	0	0
44	266	265	264	262	261	261	261	262	262	263	264	0	0	0	0	0
48	267	267	266	264	264	263	265	265	266	267	268	0	0	0	0	0
52	263	262	262	262	261	261	262	262	264	264	265	0	0	0	0	0
56	260	260	260	259	259	260	259	261	261	262	263	262	261	261	261	260
60	252	251	252	252	252	251	252	252	253	255	254	254	255	255	255	255
64	242	241	241	241	239	239	240	240	241	243	243	244	245	245	246	246
68	230	230	228	227	226	226	226	227	228	229	230	232	232	234	235	236
72	213	213	211	210	212	213	212	214	215	215	217	219	218	221	222	221
76	197	197	196	198	199	202	203	204	204	205	206	208	207	209	211	209
80	191	190	192	196	197	199	199	198	200	203	202	203	202	201	202	202
84	200	199	199	204	204	206	204	201	200	199	198	198	196	196	197	198
88	220	217	214	219	218	216	215	211	202	197	195	199	195	193	196	195
92	223	221	220	214	218	210	210	206	202	201	195	195	193	191	186	184

MAY

SOUTH LATITUDE

ALT.	75	70	65	60	55	50	45	40	35	30	25	20	15	10	5	0
40	0	0	0	0	0	0	235	239	243	247	251	253	254	254	254	253
44	0	0	0	0	0	0	245	249	253	257	259	260	261	262	261	264
48	0	0	0	0	0	0	251	255	259	263	264	265	266	266	263	266
52	0	0	0	0	0	0	253	254	257	260	261	262	262	263	261	263
56	0	0	0	0	0	249	250	252	253	255	256	257	258	258	259	260
60	0	0	0	0	0	240	246	244	245	247	248	249	249	249	250	252
64	0	0	0	0	0	240	240	235	235	235	235	236	236	237	238	239
68	0	0	0	0	0	240	233	228	225	224	223	223	224	224	225	224
72	0	0	0	0	0	228	224	221	213	212	210	211	211	209	210	209
76	0	0	0	0	0	218	213	213	205	201	200	201	203	202	202	202
80	0	0	0	0	0	215	211	210	206	200	199	198	199	201	200	201
84	0	0	0	0	0	219	218	214	212	209	206	202	200	200	198	198
88	0	0	0	0	0	227	227	221	219	219	211	205	203	203	202	200
92	0	0	0	0	0	218	226	225	224	219	214	208	207	205	210	208

NORTH LATITUDE

ALT.	0	5	10	15	20	25	30	35	40	45	50	55	60	65	70	75
40	253	254	255	255	254	254	254	255	257	258	259	0	0	0	0	0
44	264	263	263	263	262	261	263	264	266	267	268	0	0	0	0	0
48	266	265	264	263	263	264	266	267	269	270	272	0	0	0	0	0
52	263	262	262	262	261	262	264	265	266	268	269	0	0	0	0	0
56	260	260	260	260	260	261	262	263	264	265	267	269	271	272	273	274
60	252	252	254	254	253	253	255	255	256	257	258	260	262	264	265	267
64	239	239	239	239	240	239	240	241	242	244	246	248	251	252	254	255
68	224	223	222	222	224	224	223	225	226	228	230	233	236	237	240	241
72	209	208	207	207	207	207	206	209	209	211	213	216	218	221	222	222
76	202	202	200	199	198	196	196	195	195	195	197	200	201	203	204	203
80	201	199	201	201	200	197	195	190	189	185	184	186	188	187	187	189
84	198	198	204	205	206	204	200	194	188	184	178	176	175	173	173	175
88	200	202	208	211	211	212	207	205	196	190	182	179	171	167	166	162
92	208	212	207	209	204	209	200	200	198	191	189	185	180	180	175	170

JUNE

SOUTH LATITUDE

ALT.	75	70	65	60	55	50	45	40	35	30	25	20	15	10	5	0
40	0	0	0	0	0	0	233	238	244	248	251	252	252	251	250	250
44	0	0	0	0	0	0	246	250	256	259	260	260	259	259	259	259
48	0	0	0	0	0	0	253	257	261	264	264	264	263	263	261	260
52	0	0	0	0	0	0	256	257	260	261	261	261	261	261	260	259
56	0	0	0	0	0	0	248	252	255	255	256	256	257	257	258	258
60	0	0	0	0	0	0	245	245	247	246	246	247	248	249	249	250
64	0	0	0	0	0	0	242	236	234	233	233	233	235	236	236	237
68	0	0	0	0	0	0	236	224	219	218	219	221	223	225	225	224
72	0	0	0	0	0	0	231	214	207	206	207	211	212	213	213	212
76	0	0	0	0	0	0	223	211	203	199	200	202	204	206	207	207
80	0	0	0	0	0	0	211	215	209	202	200	196	198	201	202	201
84	0	0	0	0	0	0	212	218	219	215	207	199	195	194	195	194
88	0	0	0	0	0	0	228	225	229	226	214	209	197	192	196	194
92	0	0	0	0	0	0	229	237	230	222	214	206	201	198	194	200

NORTH LATITUDE

ALT.	0	5	10	15	20	25	30	35	40	45	50	55	60	65	70	75
40	250	252	250	250	251	252	254	255	256	258	259	0	0	0	0	0
44	259	260	259	259	259	260	261	263	264	267	268	0	0	0	0	0
48	260	261	262	262	263	265	265	266	268	270	272	0	0	0	0	0
52	259	259	260	260	261	262	263	264	266	268	271	0	0	0	0	0
56	258	259	259	259	258	259	261	263	265	267	269	274	0	0	0	0
60	250	251	251	251	250	250	251	254	256	259	261	265	0	0	0	0
64	237	238	237	236	235	235	236	239	241	245	248	252	0	0	0	0
68	224	224	222	222	221	221	221	223	225	228	232	235	0	0	0	0
72	212	210	209	209	209	209	208	208	207	209	212	215	0	0	0	0
76	207	205	204	204	205	203	202	196	194	193	194	196	0	0	0	0
80	201	201	201	203	202	197	197	189	186	182	177	178	0	0	0	0
84	194	194	197	198	197	194	192	186	181	174	166	161	0	0	0	0
88	194	194	198	198	197	203	199	194	182	177	171	160	0	0	0	0
92	200	202	197	198	200	200	198	195	190	188	182	182	0	0	0	0

JULY

SOUTH LATITUDE

ALT.	75	70	65	60	55	50	45	40	35	30	25	20	15	10	5	0
40	0	0	0	0	0	0	244	246	249	250	251	250	249	248	247	244
44	0	0	0	0	0	0	254	256	258	258	259	258	258	258	257	257
48	0	0	0	0	0	0	258	259	261	262	262	262	263	263	263	262
52	0	0	0	0	0	0	258	257	258	259	260	260	261	261	262	262
56	0	0	0	0	0	0	254	253	254	255	255	256	256	257	258	259
60	0	0	0	0	0	0	247	245	245	246	246	248	247	249	250	250
64	0	0	0	0	0	0	234	229	229	231	233	235	236	237	239	239
68	0	0	0	0	0	0	222	215	215	216	220	224	226	227	228	228
72	0	0	0	0	0	0	216	208	205	204	208	211	216	218	217	216
76	0	0	0	0	0	0	214	207	203	200	202	203	207	209	208	207
80	0	0	0	0	0	0	218	213	208	205	201	199	197	198	198	200
84	0	0	0	0	0	0	226	222	219	213	206	201	193	192	193	193
88	0	0	0	0	0	0	230	230	226	218	212	207	198	193	193	192
92	0	0	0	0	0	0	232	232	228	219	213	208	207	201	198	198

NORTH LATITUDE

ALT.	0	5	10	15	20	25	30	35	40	45	50	55	60	65	70	75
40	244	245	247	248	250	251	252	253	255	256	258	0	0	0	0	0
44	257	258	259	258	258	259	260	261	263	264	266	0	0	0	0	0
48	262	263	263	261	262	263	264	265	266	268	270	0	0	0	0	0
52	262	262	261	261	261	261	261	262	264	266	268	0	0	0	0	0
56	259	260	260	260	257	256	256	258	261	263	267	271	0	0	0	0
60	250	251	252	251	249	249	246	249	251	255	257	261	0	0	0	0
64	239	239	238	237	237	235	233	234	236	241	243	246	0	0	0	0
68	228	227	225	224	224	223	223	221	221	223	226	229	0	0	0	0
72	216	215	212	211	212	212	211	208	206	205	206	209	0	0	0	0
76	207	207	205	205	205	206	202	201	198	191	190	191	0	0	0	0
80	200	201	202	202	201	197	191	193	190	184	180	176	0	0	0	0
84	193	195	198	198	197	194	191	188	185	180	173	164	0	0	0	0
88	192	194	195	200	200	201	202	195	193	185	177	167	0	0	0	0
92	198	199	195	197	201	199	198	195	194	191	185	184	0	0	0	0

AUGUST

SOUTH LATITUDE

ALT.	75	70	65	60	55	50	45	40	35	30	25	20	15	10	5	0
40	0	0	0	0	0	246	247	249	251	252	251	250	249	248	247	245
44	0	0	0	0	0	255	256	257	259	260	260	259	259	259	261	262
48	0	0	0	0	0	259	259	260	261	262	263	263	264	265	267	267
52	0	0	0	0	0	257	255	255	257	258	259	260	262	263	264	263
56	0	0	0	0	258	254	251	250	252	254	256	256	257	258	259	259
60	0	0	0	0	253	247	243	241	244	246	248	249	249	250	252	252
64	0	0	0	0	243	237	231	228	229	232	235	237	238	240	242	240
68	0	0	0	0	233	228	221	216	217	218	222	225	227	230	230	229
72	0	0	0	0	225	220	213	207	207	206	209	212	216	215	216	216
76	0	0	0	0	218	214	212	208	204	203	202	204	205	204	206	206
80	0	0	0	0	213	213	218	219	212	208	204	201	197	198	197	196
84	0	0	0	0	216	221	225	226	220	215	211	203	198	195	190	193
88	0	0	0	0	224	227	228	227	222	220	217	212	206	202	200	201
92	0	0	0	0	225	227	226	228	225	222	219	220	216	217	218	217

NORTH LATITUDE

ALT.	0	5	10	15	20	25	30	35	40	45	50	55	60	65	70	75
40	245	245	247	248	248	248	249	250	251	252	253	0	0	0	0	0
44	262	262	261	258	257	256	256	258	259	260	261	0	0	0	0	0
48	267	266	265	262	260	259	260	260	262	263	265	0	0	0	0	0
52	263	263	262	261	260	259	259	259	260	261	263	0	0	0	0	0
56	259	260	261	261	259	257	256	255	257	259	262	267	270	272	0	0
60	252	253	254	253	252	251	250	248	248	250	252	256	260	263	0	0
64	240	241	241	240	240	240	237	234	235	237	238	241	245	249	0	0
68	229	228	226	226	225	227	224	223	221	222	222	224	228	233	0	0
72	216	215	212	213	210	212	214	212	210	208	205	207	208	215	0	0
76	206	205	203	205	202	202	207	204	201	197	193	191	189	197	0	0
80	196	198	200	201	202	198	203	199	196	190	187	181	179	181	0	0
84	193	194	197	200	203	202	201	199	196	189	187	180	174	166	0	0
88	201	203	203	209	207	209	208	204	206	199	194	189	180	167	0	0
92	217	219	214	211	210	204	203	202	203	202	200	199	198	193	0	0

SEPTEMBER

SOUTH LATITUDE

ALT.	75	70	65	60	55	50	45	40	35	30	25	20	15	10	5	0
40	0	0	0	0	0	253	252	251	252	253	252	253	253	252	254	0
44	0	0	0	0	0	262	260	260	261	262	261	261	262	263	261	0
48	0	0	0	0	0	265	263	263	263	264	264	264	265	266	264	0
52	0	0	0	0	0	261	259	258	259	259	260	261	262	263	263	0
56	0	266	261	259	257	254	252	253	255	256	256	257	257	257	259	258
60	0	257	254	252	249	246	245	245	247	249	249	250	250	249	250	251
64	0	246	244	242	238	235	233	232	232	234	235	238	240	240	240	241
68	0	237	235	231	229	226	223	220	219	219	221	225	229	230	230	230
72	0	227	225	222	221	219	217	213	212	209	210	212	215	216	216	215
76	0	218	218	217	216	217	215	214	212	208	206	205	204	203	201	199
80	0	216	214	214	216	217	214	213	212	208	208	203	198	193	192	191
84	0	220	214	216	217	215	214	215	212	210	208	205	199	194	196	194
88	0	220	220	225	219	218	218	220	218	218	215	215	212	211	210	209
92	0	213	219	222	219	219	216	217	218	217	220	219	220	225	228	234

NORTH LATITUDE

ALT.	0	5	10	15	20	25	30	35	40	45	50	55	60	65	70	75
40	0	0	0	248	248	246	247	247	248	249	250	0	0	0	0	0
44	0	0	0	265	262	259	259	258	258	259	259	0	0	0	0	0
48	0	0	0	267	264	262	262	262	262	262	263	0	0	0	0	0
52	0	0	0	261	260	259	258	258	258	259	259	0	0	0	0	0
56	258	260	260	258	257	257	256	255	255	255	256	257	257	261	260	260
60	251	252	252	253	251	251	249	248	246	245	247	249	248	252	253	256
64	241	241	241	241	239	238	238	236	234	233	233	236	236	238	242	245
68	230	227	227	227	226	224	224	223	223	221	219	221	222	224	227	229
72	215	214	213	214	213	211	211	209	210	209	207	206	208	210	210	213
76	199	204	203	204	203	200	202	203	203	201	200	196	198	198	198	200
80	191	196	197	197	197	199	201	204	205	203	202	196	194	193	194	191
84	194	197	197	198	199	206	207	208	207	206	207	204	197	196	194	188
88	209	212	211	212	214	211	213	210	206	207	210	217	205	201	197	191
92	234	224	227	225	225	217	213	211	211	211	209	210	209	209	206	203

OCTOBER

SOUTH LATITUDE

ALT.	75	70	65	60	55	50	45	40	35	30	25	20	15	10	5	0
40	0	0	0	0	0	253	254	255	255	256	255	253	258	259	259	0
44	0	0	0	0	0	264	265	266	266	265	265	264	264	266	267	0
48	0	0	0	0	0	271	271	270	269	267	265	265	263	264	266	0
52	0	0	0	0	0	268	267	265	264	262	260	259	259	261	262	0
56	272	269	268	265	264	261	259	258	258	258	257	255	256	257	258	257
60	266	263	261	260	258	255	254	253	251	251	250	250	249	248	249	249
64	254	253	250	249	247	243	243	242	239	239	238	238	238	238	239	238
68	240	240	239	236	233	232	230	229	226	226	225	224	225	225	226	225
72	225	226	226	223	220	220	218	217	215	212	211	209	210	209	208	209
76	213	212	212	213	211	210	209	208	203	201	199	199	198	198	195	196
80	204	204	203	205	206	205	204	203	199	200	198	200	200	200	196	197
84	197	199	200	199	201	202	202	204	206	209	208	210	209	207	209	209
88	197	198	199	201	203	203	205	212	215	220	221	217	215	214	220	222
92	192	193	194	200	202	202	204	210	213	217	221	217	225	225	226	229

NORTH LATITUDE

ALT.	0	5	10	15	20	25	30	35	40	45	50	55	60	65	70	75
40	0	0	0	0	0	0	246	243	242	242	240	0	0	0	0	0
44	0	0	0	0	0	0	261	258	256	254	252	0	0	0	0	0
48	0	0	0	0	0	0	262	262	261	259	257	0	0	0	0	0
52	0	0	0	0	0	0	257	257	256	255	255	0	0	0	0	0
56	257	256	255	257	257	255	254	253	252	252	250	251	251	249	251	0
60	249	248	247	248	248	247	247	244	244	243	242	246	248	250	251	0
64	238	237	236	236	236	237	237	235	234	234	235	239	239	244	247	0
68	225	225	224	223	222	223	224	225	224	224	227	231	229	236	240	0
72	209	210	209	209	207	209	210	211	212	214	219	222	226	227	229	0
76	196	198	200	200	199	199	200	201	204	207	206	213	219	217	221	0
80	197	198	200	200	201	200	200	201	203	207	201	203	205	210	218	0
84	209	207	204	205	207	209	208	210	209	209	212	206	209	209	215	0
88	222	216	216	220	215	216	218	219	218	212	214	218	217	213	216	0
92	229	227	230	227	224	226	223	221	222	218	226	223	212	217	202	0

NOVEMBER

SOUTH LATITUDE

ALT.	75	70	65	60	55	50	45	40	35	30	25	20	15	10	5	0
40	0	0	0	0	0	262	262	260	259	257	255	256	254	257	257	255
44	0	0	0	0	0	272	272	272	270	268	266	264	265	266	265	265
48	0	0	0	0	0	276	275	274	271	269	267	263	264	264	263	265
52	0	0	0	0	0	272	270	268	265	265	261	260	260	260	260	261
56	278	277	274	271	271	266	265	264	261	260	259	258	258	258	258	257
60	270	268	265	263	262	260	258	256	254	252	251	250	250	248	249	247
64	259	256	254	252	249	247	246	243	242	238	238	238	238	237	238	237
68	244	244	241	238	235	232	231	228	226	224	224	226	224	224	223	224
72	227	227	225	221	218	216	214	211	208	210	208	213	209	209	209	210
76	211	208	208	205	203	200	199	197	196	201	200	196	199	200	203	204
80	195	193	192	192	192	190	191	192	194	199	203	194	201	203	204	202
84	178	178	177	181	184	186	194	194	200	204	211	214	213	212	210	203
88	167	168	170	176	184	190	200	202	209	213	217	218	221	217	216	212
92	164	166	173	177	188	196	194	207	212	211	212	215	215	217	217	225

NORTH LATITUDE

ALT.	0	5	10	15	20	25	30	35	40	45	50	55	60	65	70	75
40	255	254	253	0	247	245	243	241	238	0	0	0	0	0	0	0
44	265	264	263	0	260	257	254	251	248	0	0	0	0	0	0	0
48	265	264	263	0	263	261	258	256	253	0	0	0	0	0	0	0
52	261	261	260	0	258	256	255	254	253	0	0	0	0	0	0	0
56	257	258	258	257	256	255	253	253	253	252	253	0	0	0	0	0
60	247	247	247	246	247	247	246	247	249	245	247	0	0	0	0	0
64	237	235	235	234	235	235	238	238	240	239	239	0	0	0	0	0
68	224	224	223	223	222	223	227	229	231	233	231	0	0	0	0	0
72	210	212	211	211	210	212	213	217	218	223	224	0	0	0	0	0
76	204	206	205	203	202	201	203	205	208	212	216	0	0	0	0	0
80	202	204	203	203	202	199	201	202	208	208	215	0	0	0	0	0
84	203	205	205	206	210	210	212	210	213	212	216	0	0	0	0	0
88	212	210	213	210	214	219	226	223	220	225	218	0	0	0	0	0
92	225	224	221	220	218	219	219	222	222	223	224	0	0	0	0	0

DECEMBER

SOUTH LATITUDE

ALT.	75	70	65	60	55	50	45	40	35	30	25	20	15	10	5	0
40	0	0	0	0	0	264	263	261	258	255	252	250	249	248	247	246
44	0	0	0	0	0	272	272	270	268	265	263	261	260	259	256	254
48	0	0	0	0	0	277	275	272	270	267	265	263	262	261	261	260
52	0	0	0	0	0	274	272	269	266	263	261	261	260	262	261	261
56	0	0	0	0	276	271	269	266	264	261	259	258	259	261	261	261
60	0	0	0	0	266	263	261	257	255	251	251	249	250	253	252	253
64	0	0	0	0	253	249	246	243	240	237	236	238	239	242	243	243
68	0	0	0	0	237	233	229	227	224	223	222	226	226	228	230	231
72	0	0	0	0	217	214	212	209	209	211	212	214	214	214	216	216
76	0	0	0	0	200	196	196	198	199	202	207	208	209	207	208	206
80	0	0	0	0	185	184	185	195	196	199	205	209	209	207	205	202
84	0	0	0	0	172	178	184	193	195	201	203	208	208	208	204	200
88	0	0	0	0	167	179	188	191	195	203	207	205	204	208	208	200
92	0	0	0	0	176	180	185	189	199	201	204	200	204	203	207	204

NORTH LATITUDE

ALT.	0	5	10	15	20	25	30	35	40	45	50	55	60	65	70	75
40	246	246	247	245	246	246	244	240	237	0	0	0	0	0	0	0
44	254	254	254	256	255	255	253	249	245	0	0	0	0	0	0	0
48	260	259	259	260	259	259	258	255	249	0	0	0	0	0	0	0
52	261	261	261	260	258	258	256	253	248	0	0	0	0	0	0	0
56	261	260	260	258	258	256	255	253	250	249	251	0	0	0	0	0
60	253	251	250	249	247	247	245	244	243	243	246	0	0	0	0	0
64	243	242	241	239	236	235	232	232	232	233	238	0	0	0	0	0
68	231	232	232	231	228	224	221	220	222	224	230	0	0	0	0	0
72	216	218	221	220	219	215	213	212	217	219	224	0	0	0	0	0
76	206	207	209	211	211	208	208	210	214	218	221	0	0	0	0	0
80	202	200	201	201	203	204	211	214	209	219	223	0	0	0	0	0
84	200	197	199	199	202	208	213	219	215	221	225	0	0	0	0	0
88	200	198	200	204	203	212	214	223	229	233	228	0	0	0	0	0
92	204	205	203	202	202	207	218	224	236	235	227	0	0	0	0	0